



UNIVERSIDAD  
**NACIONAL**  
DE COLOMBIA

# **Friction Stir Welding (FSW) process evaluation of aluminum Tie components used in the door mechanism of MAN trains.**

**Santiago Escobar Muñoz**

Universidad Nacional de Colombia  
Facultad de Minas, Departamento de Ingeniería  
Medellín, Colombia  
2021



# **Friction Stir Welding (FSW) process evaluation of aluminum Tie components used in the door mechanism of MAN trains.**

**Santiago Escobar Muñoz**

Research work presented as requirement to qualify for the title of:

**Master's in Mechanical Engineering**

Director:

Ph. D. Diana María López Ochoa

Co-director:

Ph. D. Elizabeth Hoyos Pulgarín

Line of investigation:

Manufacturing processes

Universidad Nacional de Colombia  
Facultad de Minas, Departamento de Ingeniería  
Medellín, Colombia

2021



*Dedication*

*To my parents*



## **Acknowledgements**

I like to express my most sincere gratitude to Elizabeth Hoyos Pulgarín for always being a fundamental part of my formation as engineer and as a human being, working tirelessly and selflessly to help me solve all the problems and providing viable solutions, and helping to obtain the crucial funding to complete every stage. To Diana Lopez Ochoa for the guidance and new perspectives provided that finally enriched my project and life, giving me new perceptions during this process. I will be deeply grateful all my life and proud to say, “I worked with them”.

Also, I thank the Royal Academy of Engineering for letting me be part of the IAPP18-19\266 “Implementation of friction stir welding (FSW) in the Colombian rail transport sector” project in which my thesis was carried out and for the funding provided to the local development in conjunction with TWI as technical partner, and to Jeroen De Backer and Jhonnatan Martin for their knowledge sharing. Additionally, I like to thank to Sapiencia (local public fund), for the economic support given during this process and to the department of mechanical engineering of the Universidad Nacional de Colombia for the financial aid given and for letting me be part of the institution.

Thanks to the Metro de Medellin, to the engineers Mauricio Enrico Palacio and Diego Alejandro Vélez, for letting me enter to their facilities and providing me with all the information needed and for being kind with all the requests made during this time.

Finally and not less important, thanks to professor Yesid Montoya Goéz and the welding research group of Universidad EIA for the time spent, dedication and recomendations during this process.





## Abstract

This project is focused in the development of a welding procedure using the Friction Stir Welding (FSW) process as an alternative for the local manufacture of components using lightweight materials without requiring great investment in specialized machinery. As case of study, a structural aluminum piece called “Tie” used in the railway cars owned by Metro de Medellín was selected and evaluated using analytical and computational tools to propose a viable alternative in accordance with the process, accessible materials and mechanical requirements.

A prototype was successfully design and constructed according to the FSW proposed procedure, using the aluminum alloy AA6082 – T4 as base material, and after 5 months of operation and more than 1540 cycles, the *tie* does not present any problem or discontinuities which could jeopardize its mechanical performance; finally validating the possible usage of FSW as manufacturing alternative and giving a chart for future developments.

The project was aligned with the results with a major plan called “Implementation of friction stir welding (FSW) in the Colombian rail transport sector” funded by the Royal Academy of Engineering and technically supported by TWI.

Palabras clave: Friction Stir Welding, railway, welding, aluminum.

## Resumen

### *Título del trabajo en español*

### ***Evaluación del proceso de soldadura Friction Stir Welding (FSW) en componentes traviesa de aluminio usados en el mecanismo de puertas de trenes MAN***

Este proyecto está enfocado en el desarrollo de un procedimiento de soldadura usando Friction Stir Welding (FSW) o también conocido como soldadura por fricción y agitación, para la fabricación local de componentes usando aleaciones ligeras y sin requerir grandes inversiones monetarias para la compra de maquinaria especializada. Como caso de estudio se seleccionó un componente estructural de aluminio llamado “Traviesa” y que es usado en los vagones ferroviarios del Metro de Medellín.

Dicho componente fue evaluado usando herramientas computacionales y analíticas para así proponer una alternativa viable de manufactura teniendo en cuenta el proceso de soldadura, los materiales localmente disponibles y los requerimientos mecánicos.

Finalmente, se diseñó y fabricó un prototipo funcional de acuerdo con el procedimiento de soldadura propuesto, usando la aleación comercial de aluminio AA 6082 - T4 como material base, el cual fue evaluado durante 5 meses de operación que se traducen en 1540 ciclos; sin presentar ningún inconveniente o discontinuidad que ponga en riesgo su operación.

Todo lo anteriormente presentado permitió evaluar y aumentar la confianza de utilización de FSW como alternativa de manufactura, y ser referente adecuado para futuros desarrollos.

Los resultados del proyecto están alineados a una propuesta mayor financiada por la Real Academia de Ingeniería del Reino Unido y que fue apoyada técnicamente por TWI y que

tiene por título “Implementation of friction stir welding (FSW) in the Colombian rail transport sector”.

Palabras claves: Friction Stir Welding, transporte ferroviario, soldadura, aluminio.



---

## Index

<b>1. Introduction .....</b>	<b>1</b>
<b>2. Problem statement .....</b>	<b>3</b>
<b>3. Objectives .....</b>	<b>5</b>
<b>3.1 General objective .....</b>	<b>5</b>
<b>3.2 Specific objective.....</b>	<b>5</b>
<b>4. Framework .....</b>	<b>6</b>
<b>4.1 Introduction to the Friction Stir Welding (FSW) technique.....</b>	<b>6</b>
<b>4.2 Weld discontinuities by arc processes .....</b>	<b>8</b>
□ Porosities in aluminum .....	8
□ Solidification cracking.....	8
□ Segregation cracking.....	9
<b>4.3 Comparison between techniques .....</b>	<b>9</b>
<b>4.4 Regulation.....</b>	<b>12</b>
<b>4.5 Industrial Background.....</b>	<b>17</b>
<b>5. Methodology .....</b>	<b>20</b>
<b>5.1 Specific objective 1 goals .....</b>	<b>20</b>
<b>5.2 Specific objective 2 goals .....</b>	<b>21</b>
<b>5.3 Specific objective 3 goals .....</b>	<b>22</b>
<b>5.4 Bibliographical research .....</b>	<b>23</b>
<b>5.5 Results.....</b>	<b>23</b>

---

<b>6. Results</b> .....	<b>24</b>
<b>6.1 Construction and operational requirements for the tie</b> .....	<b>24</b>
6.1.1 Tie's description .....	24
6.1.2 Maintenance records .....	26
6.1.3 General geometry .....	27
6.1.4 Discontinuities and assessment .....	28
6.1.5 CAD models .....	29
6.1.6 Identification of the base metal .....	30
6.1.7 Free body diagram .....	31
6.1.8 FEA analysis .....	34
6.1.9 Stress critical path .....	43
<b>6.2 Fabrication of the Tie by FSW</b> .....	<b>46</b>
6.2.1 Manufacturing considerations .....	46
6.2.2 Material selection .....	47
6.2.3 Design considerations .....	47
6.2.4 Fixing and welding .....	53
6.2.5 Forces during welding .....	58
<b>6.3 Evaluation of welded samples</b> .....	<b>61</b>
6.3.1 Samples and hardness evaluation .....	61
6.3.2 Hardness .....	62
6.3.3 Prototype component .....	65
6.3.4 Prototype inspection .....	66
<b>6.4 Welding procedure</b> .....	<b>68</b>
<b>7. Conclusions</b> .....	<b>71</b>
<b>8. References</b> .....	<b>73</b>

## Figure list

<b>Figure 1.</b> Railway lines by 2035 in Colombia [4] .....	1
<b>Figure 2.</b> Component selected and located at the door mechanism. ....	3
<b>Figure 3.</b> FSW schematic, a) Welding model and b) Tool closeup (own elaboration). ....	6
<b>Figure 4.</b> Lack of penetration on welds [24]. ....	7
<b>Figure 5.</b> Porosity example [30]. ....	8
<b>Figure 6.</b> Solidification cracking [30]. ....	9
<b>Figure 7.</b> Segregation crack on AA7075 – T6 [10]. ....	9
<b>Figure 8.</b> FSW Weld microstructure AA 7075 – T6 [34]. ....	10
<b>Figure 9.</b> Friction Stir Welding zones [36] .....	10
<b>Figure 10.</b> Left images, MIG welds on aluminum. Right images, FSW process [28] .....	11
<b>Figure 11.</b> Japanese bullet train made by FSW [43] .....	17
<b>Figure 12.</b> HITACHI trains using FSW [44]. ....	17
<b>Figure 13.</b> Alstom LHB trains made using FSW [45]. ....	18
<b>Figure 14.</b> Configuration of weld [46]. ....	18
<b>Figure 15.</b> Bobbing tool for extruded profiles [48] .....	19
<b>Figure 16.</b> Methodology proposed. ....	20
<b>Figure 17.</b> Tie's location, a) door assembly, b) mechanism assembly, c) mobile mechanism backbone and d) tie. ....	24
<b>Figure 18.</b> Mechanism assembly, from left to right: Tie, Support body and rail .....	25
<b>Figure 19.</b> Displacement of the components. a) assembly when the door is closed, b) assembly when the door is open .....	25
<b>Figure 20.</b> CAD models of the ties. At left the original, at right the locally manufactured. On the side a zoom of the differences at the ties. ....	27
<b>Figure 21.</b> Original weld locations. ....	27
<b>Figure 22.</b> Presence of discontinuities around the tie .....	29
<b>Figure 23.</b> Images of CAD models, a) Original Tie, b) Locally made Tie and c) Door mechanism. ....	30

---

<b>Figure 24.</b> Component selected – tie.....	31
<b>Figure 25.</b> Free body diagram .....	32
<b>Figure 26.</b> Transversal subdivision.....	33
<b>Figure 27.</b> FEA constrains and considerations.....	34
<b>Figure 28.</b> Open mechanism - Original piece.....	35
<b>Figure 29.</b> Open mechanism - locally manufactured.....	36
<b>Figure 30.</b> Closed mechanism – Original piece.....	37
<b>Figure 31.</b> Closed mechanism - locally manufactured .....	37
<b>Figure 32.</b> a) Locally made component, b) Original piece .....	38
<b>Figure 33.</b> Bracket region stress.....	39
<b>Figure 34.</b> Cracks in the components related with stress. ....	40
<b>Figure 35.</b> Heat affected zone discontinuities .....	41
<b>Figure 36.</b> Rotation from the ties .....	41
<b>Figure 37.</b> Convergence curves.....	42
<b>Figure 38.</b> Geometry constrains. ....	43
<b>Figure 39.</b> Load path identification at the ties.....	44
<b>Figure 40.</b> Distribution along tie .....	44
<b>Figure 41.</b> Comparison of the bracket.....	45
<b>Figure 42.</b> Comparison of a Tie section.....	45
<b>Figure 43.</b> Features identified for the manufacturing process. ....	46
<b>Figure 44.</b> a) “L” profile and plate, b) two “L” profiles and c) three plates.....	48
<b>Figure 45.</b> L- Shaped profiles .....	48
<b>Figure 46.</b> Types of brackets .....	49
<b>Figure 47.</b> From left to right: Insert, location and manufactured piece. ....	50
<b>Figure 48.</b> Lid models for assembly, a) Type 1 of mechanized lid, b) Type 2 of mechanized model and c) Modular type of lid. ....	51
<b>Figure 49.</b> Final Lid proposal. a) and b) represents the final component, c) Plate and d) “C” channel for mechanical assembly. ....	51
<b>Figure 50.</b> Summary of the manufacturing possibilities for the different stages in the construction of the tie.....	52
<b>Figure 51.</b> TTI disposition .....	53
<b>Figure 52.</b> Initial tool for trials for longitudinal welds .....	54
<b>Figure 53.</b> Weld 1.....	54



---

<b>Figure 54.</b> Results and configuration of welds 2 and 3 .....	55
<b>Figure 55.</b> Final welds .....	55
<b>Figure 56.</b> Post weld schematic distortion, a) expected result b) angular distortion obtained .....	56
<b>Figure 57.</b> Tool - bracket disposition, a) tolerances needed and b) new tool. ....	56
<b>Figure 58.</b> Backing design .....	57
<b>Figure 59.</b> Welds for the bracket, a) plate pattern and b) Tie welds .....	57
<b>Figure 60.</b> Bracket welds, a) plate seams, b) back of the pattern.....	58
<b>Figure 61.</b> Weld 4 micrograph made by FSW, scale 5 mm. ....	61
<b>Figure 62.</b> Samples obtained from Bracket weld .....	61
<b>Figure 63.</b> Detailed microstructure of bracket weld by FSW, scale 1000 $\mu\text{m}$ .....	62
<b>Figure 64.</b> Hardness indentations.....	63
<b>Figure 65.</b> Vickers hardness pattern on the x axis and welds samples evaluated .....	63
<b>Figure 66.</b> Tie prototype.....	65
<b>Figure 67.</b> Tie installation at wagon.....	66
<b>Figure 68.</b> Deformation .....	67
<b>Figure 69.</b> DP examination, a) general inspection, b) closeup of the Bracket and c) closeup of the Lid .....	67

---

## Table list

<b>Table 1.</b> Usual joint configurations for FSW [22] .....	12
<b>Table 2.</b> ISO requirements [40] .....	13
<b>Table 3.</b> Defects and acceptance [40] .....	14
<b>Table 4.</b> Defects and acceptance (continued) [40] .....	15
<b>Table 5.</b> AWS requirements for FSW [25] .....	16
<b>Table 6.</b> AWS acceptance criteria [41] .....	16
<b>Table 7.</b> Tie maintenance data .....	26
<b>Table 8.</b> Chemical composition of the original ties .....	30
<b>Table 9.</b> Manual calculations .....	33
<b>Table 10.</b> Aluminum comparison [62][63][66] .....	47
<b>Table 11.</b> Welding parameters Welds 1-5 .....	58
<b>Table 12.</b> Local industries [67] .....	59
<b>Table 13.</b> Welding Procedure Qualification Record for Friction Stir Welding – longitudinal weld .....	69
<b>Table 14.</b> Welding Procedure Qualification Record for Friction Stir Welding – Bracket weld .....	70

## **Annex list**

**Annex 1.** OTT-130 for manufacturing Ties

**Annex 2.** Blueprint used in OTT-130

**Annex 3.** Tie's chemical composition

**Annex 4.** Welding steps

## Products obtained

Below are presented the academic products made during the project to enhance the visibility of the objectives proposed and the local engineering advances.

### Papers and symposium presentations

- “Case Study: Implementation of FSW in the Colombian Rail Transport Sector” in The Mineral, Metals & Materials Annual Meeting & Exhibition 2021 (TMS 2021).
- “Manufacturing Concept and Prototype for Train Component Using the FSW Process” for Journal of Manufacturing and Material Processing (JMMP), <https://doi.org/10.3390/jmmp5010019>.

### Academic literature

- First chapter of the book “Friction Stir Welding and Processing XI”, from the Springer editorial, ISBN 978-3-030-65265-4.

# 1. Introduction

Colombia has more than 500 km of operative railway infrastructure consisting of 484 km maintained by the Nation, 150 km privately used by the mining industry and 53 used as touristic lines between Bogotá and Zipaquirá [1]. In those 484 km of railways lines, the only ones working for public transportation are operated by the Metro de Medellín (Mdm) since 1995 in continuous usage, despite the approvals for the Metro de Bogotá projected to be operational by 2028 [2] and the newly approved line of the MdM [3]. All of these is a small proportion of the 3513 operative kilometers which were active back in the 1950's when *Ferrocarriles Nacionales de Colombia*, a state industry was functioning.

In 2015 the ANI (*Agencia Nacional de Infraestructura*) planned the reactivation of all the forgotten infrastructure aiming for a better mobility system, a more competitive market and a greater articulation with ground mobility like freight and last mile delivery, in periods of time of 10 years and funded by the national budget. The schedule proposed aims to have a network by 2035 as presented in Figure 1.



Figure 1. Railway lines by 2035 in Colombia [4]

This expected growth opens new possibilities for fabrication, reparation, repowering and acquisition of new vehicles [5] as a response to the projected demand for new wagons like the case of Bogota's new metro system with 23 new coaches and signed start date for the next 23 of September 2020 [2][6], the other lines in construction around the country like the newly announced Metro line of Medellín mass transit system with 13,25 km of railway lines [7][8] or the substitution of imported components, aiming for the savings in maintenance and operational costs [9]; all of which promotes the usage of the local workforce. That is why, entities like the Metro de Medellín (MdM) have demonstrated interest in the implementation of new techniques of fabrication by the local manufacturing sector, looking for lower fabrication cost of pieces, better accessibility and promoting the development of local engineering.

In the case of the wagons used by the MdM, the materials implemented in their structure are predominantly aluminum alloys from the series 5000, 6000 and 7000, due to the combination of lower weight vs. greater mechanical properties; but the lack of technology for joining them locally without problems as micro-segregation, cracks and others discontinuities related with traditional arc welding processes (SMAW, GTAW and GMAW) and cost-effectiveness, makes the repairs of specific components not adequate for the performance needed. Additionally, the local manufacturing processes in some cases are not comparable with the quality required for these applications [10], making necessary the importation of those pieces [11][12].

Derived from other friction processes, Friction Stir Welding (FSW) has been used by some European, Asian and North American railway constructors to manufacture successful welds on aluminum extrusions, achieving structures with minimum distortion and maintaining or enhancing the mechanical performance while decreasing the probability of obtaining the discontinuities mentioned before [13].

In Colombia, the technique has been primarily studied in academic applications [14]–[17] without any major use by the metal mechanic sector; which if applied and proved in this case, could not only help the railway industry but other industries to obtain better components, more suited to compete in a global economy.

## 2. Problem statement

Metro de Medellín has in its fleet two types of trains, the first batch of 43 cars was acquired back in 1995 at the beginning of the operation and the others 36, bought in 2018 as a response to the continuous demand increase in recent years linked with the population growth of the Aburra's Valley [18]. Those older wagons used today were designed in the late 1980s by a European consortium composed of three companies (MAN, SIEMENS and ATEINSA), later dissolved in 1996.

The early cars have been maintained over the years by the local operator with components left by the original manufacturer and some commercially available parts (or imported if necessary) like the bearings, seals, fiber panels, etc.; and because those wagons are reaching their design life of 30 years and 3.2 million kilometers [19], the spare parts are scarce or not made any more. Additionally, the metropolitan government approved the refurbishment of the old trains, which translates to a bigger demand for locally manufactured components.

One of those no longer available pieces is the aluminum *tie* used in the door mechanism as structural beam (shown in Figure 2) and needed in the refurbishment process mentioned before. This element is a tailor-made C channel which in recent years has been replaced because it has presented cracks after about 15 years of operation and more than  $10^6$  cycles of intermittent loading.



**Figure 2.** Component selected and located at the door mechanism.

Since the first replacement was performed (by 2012), MdM has tried to substitute the component with locally manufactured pieces to guarantee their availability and cost effectiveness for the operation of the system, but those components underperform in comparison with the original parts, needing a more frequent replacement to maintain the operational reliability, a key factor for Metro de Medellín.

The manufacturing processes used by locals to construct this piece involve arc welding methods like GMAW, GTAW, and machining; but it has been observed that the discontinuities which appear at the component are related to the heat-affected zones, neighbor areas of the welded material that suffer from changes in material properties due to high temperatures [20], and surface quality left in the base metal by those processes. Friction Stir Welding (FSW) present advantages against arc welding, such as narrower heat affected zones, better surface finish and mechanical properties. A question then appears, can the process be suited to be implemented locally to fulfil the local repairability and availability of components for the projected operation?

It is of interest to mention that this project is part of a major collaboration funded by the Newton Fund and the Royal Academy of Engineering from the UK, in which Metro de Medellín acts as the local industry partner and TWI as FWS expert (IAPP 266\18-19).



## **3.Objectives**

### **3.1 General objective**

To develop a FSW welding procedure which permits the fabrication of "Tie" components required by MAN train's door mechanism to operate with the performance needed.

### **3.2 Specific objective**

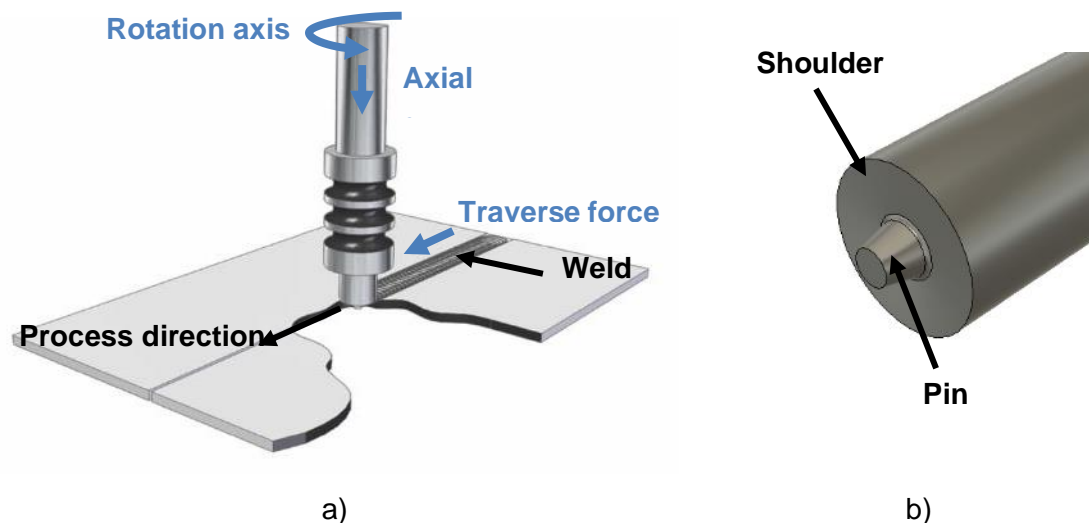
- To evaluate the construction and operational requirements of the Tie.
- To design a method of fabrication for the selected component by FSW.
- To evaluate welded samples using basic microstructural characterization and hardness testing.

## 4. Framework

### 4.1 Introduction to the Friction Stir Welding (FSW) technique

The welding technique known as Friction Stir Welding (FSW) was invented in 1991 at The Welding Institute (TWI) in the United Kingdom, as a response to the low weldability of light materials like the aluminum alloys. It consists of a non-consumable tool that advances at a constant rate perpendicularly to its rotational axis, along a seam constructed by the position of two material plates against a backing anvil [21]; one of the possible configurations is shown in Figure 3 - a.

The tool commonly used in FSW has two distinctive geometrical features (Figure 3- b), the first one is the pin, which has a slightly shorter length than the material's thickness to guarantee a complete bond; this feature oversees the mixing action along the transversal section of the weld bead. The second characteristic is the shoulder, which retains the plasticized bulk of material to guarantee the soundness of the joint accompanied by a backing anvil (backing plate) [22].

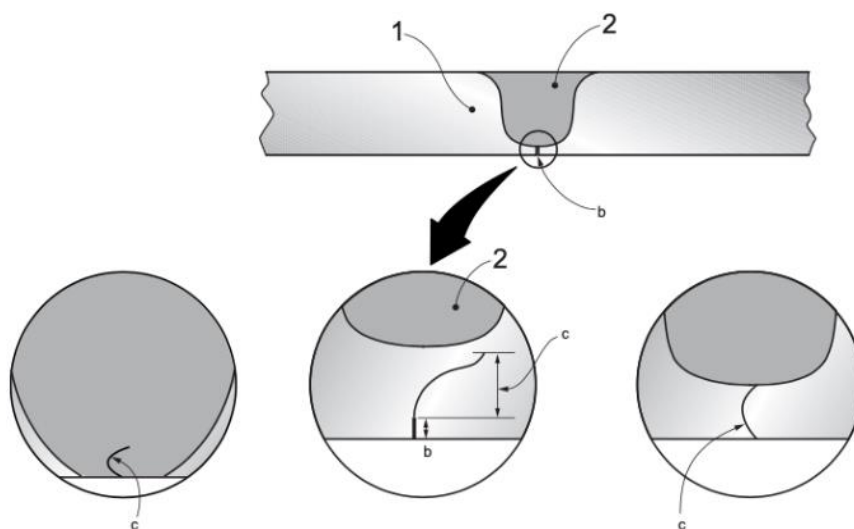


**Figure 3.** FSW schematic, a) Welding model and b) Tool closeup (own elaboration).

Initially, the tool penetrates the material in the same direction of its rotational axis until a previously tuned distance is reached, followed by an increment of temperature as result of the friction between the rotating tool and the material to be welded during for a period of time called *dwel time*, plasticizing the material. Prior to the movement along the seam, the tool is usually set to an angle (between  $0^{\circ}$  to  $3^{\circ}$  degrees) to guarantee soundness [23].

During the welding operation, the material involved in the process experiment different forces due to the motion of the tool and the required force to control its position, those are known as axial and traverse force; and because the tool rotates while advances, the plate that experiments the stir action in the same direction as the travel speed is known as advancing side and the complementary as retreating side until the weld is finished and left with an exit hole [24], [25].

Finally, FSW can present some discontinuities due to improper set-up o welding parameters which can be visible in an incomplete penetration of the pin along with the thickness of the material (Figure 4), excessive plasticization which is translated in flash along the joint [24], [25] and other less visible discontinuities (and possibly requiring destructive tests) like tunnel defects, involving a continuous or semi-continuous cavity along the seam due to improper mixing or temperatures during process and kissing bonds, related with the formation of oxides due to high transverse or low rotational speeds, finally separating the material in the stir zone [26].



**Figure 4.** Lack of penetration on welds [24].

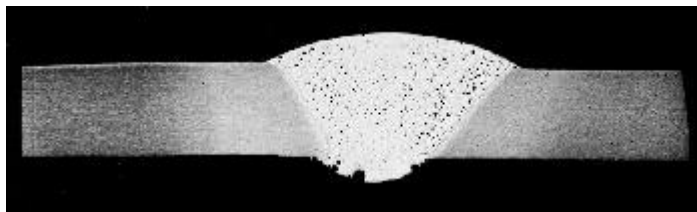
## 4.2 Weld discontinuities by arc processes

Arc welding has been used to join different aluminum alloys families, but due to the fusion of the metal a heat affected zone is always left with a high probability of inclusions and different grain structures, leading to a preferential faulty region in the material [27][28]; which can easily be translated into discontinuities [29]. Some industrial approaches exist addressing the diminution of discontinuities, like the usage of proper filler wires and pre-heating temperatures, with the guidance of standards such as the BS EN 1011 Pt 4:2000 for the most common aluminum alloys [30].

Usual discontinuities that occur with arc joining are:

- **Porosities in aluminum**

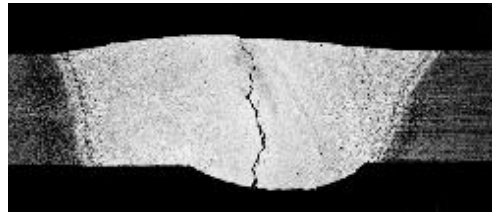
Appears during the solidification because in some cases shielding gases or air get trapped when turbulences occur in the weld pool, like what happens when low current is set up prior a fusion welding, or when large droplets are transferred and the metal is deposited faster than the rate the gases escape [31]. Other less likely reasons are hydrogen absorption by the metal because the joint is made near the presence of hydrocarbons or water, from the parent materials due to improper cleaning, wire, or a surrounding atmosphere moisture. Figure 5 presents an example of this type of discontinuities [30].



**Figure 5.** Porosity example [30].

- **Solidification cracking**

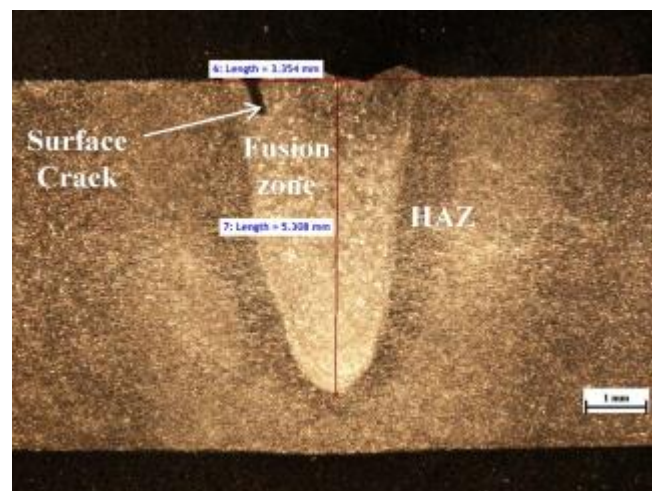
This one is the result of high stresses in the pool of molten material result in temperature differences and thermal contraction of the liquid and solid metal phases, leading to bigger tensions in the molten area. This type of cracks usually appears at the middle of the seam or at the end of the welding operation (Figure 6) [30].



**Figure 6.** Solidification cracking [30].

- **Segregation cracking**

It appears in the heat affected zone, around the grain boundaries, where the material cannot support the stresses when the metal contracts while cools down after the welding process. This happens because the alloying components form a lower melting point layer around the grains [32]. An example of this discontinuity can be observed in Figure 7, where a crack appeared on the surface by this mechanism.

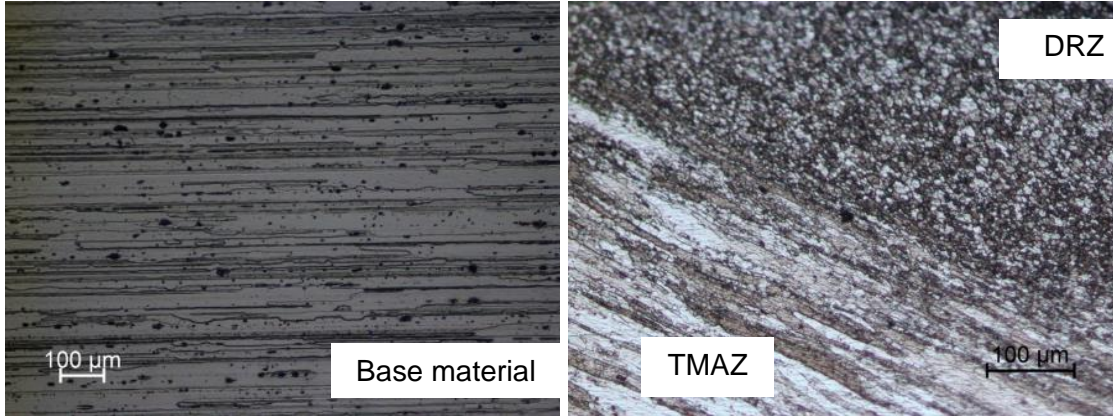


**Figure 7.** Segregation crack on AA7075 – T6 [10].

### 4.3 Comparison between techniques

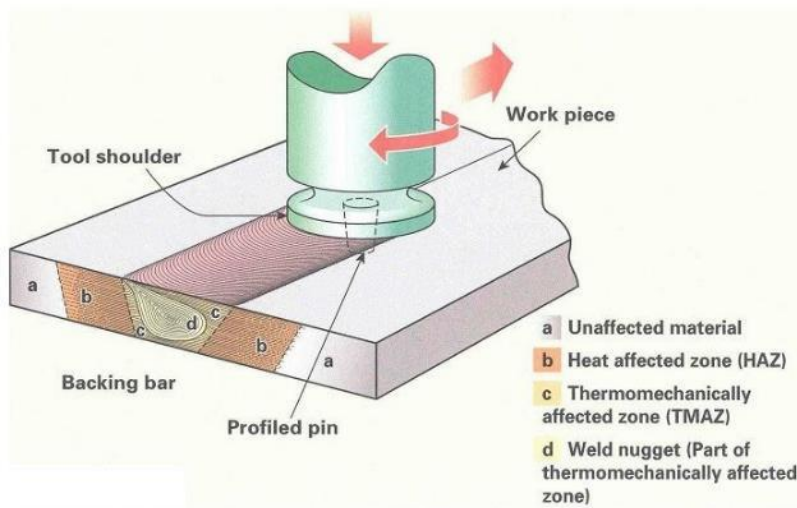
Contrary to the fusion welding, during the FSW process the material experiments a phenomenon called *dynamic recrystallization*, which decreases the grain size by shear force while the tool advances along the seam; enabling the formation of new grain boundaries and dislocations and achieving an uniform region [33]. This recrystallization can

be appreciable at the three different regions observable in Figure 8, the base material, thermo-mechanical affected zone (TMAZ) and the dynamic recrystallization zone (DRZ).



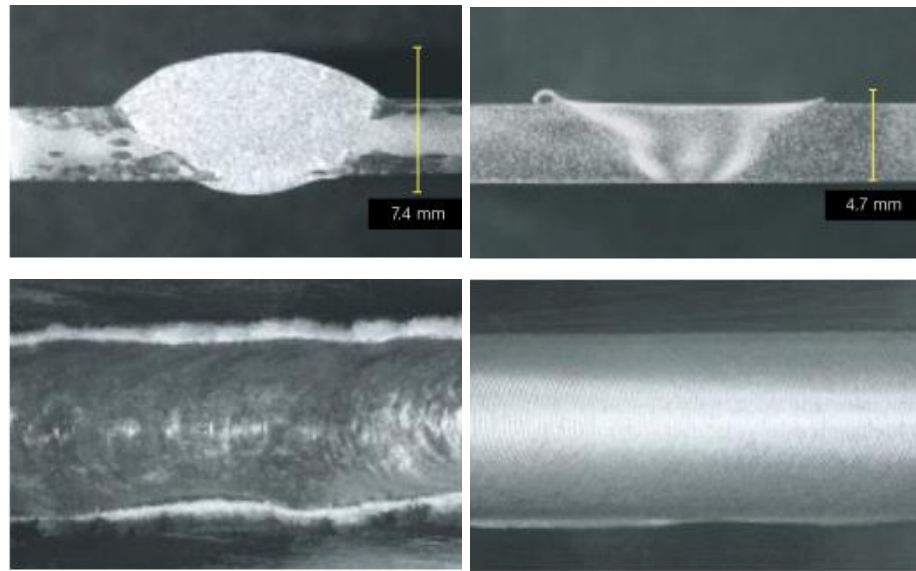
**Figure 8.** FSW Weld microstructure AA 7075 – T6 [34]

The geometrical distribution of those areas is presented in Figure 9, which is divided into four zones. The first and second are called “nugget”, where the pin mixes the material and the Thermomechanical affected zone (TMAZ), where the mixing action is supported by the shoulder; both having similar grains sizes and the dynamic recrystallization happens. The third region is the heat affected zone where the grains does not suffer from any mechanical deformation but experiment heat cycles, and finally the unaffected material or base metal [35].



**Figure 9.** Friction Stir Welding zones [36]



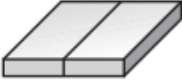



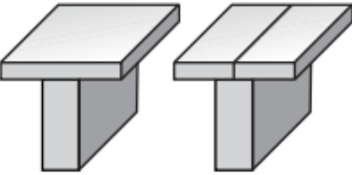
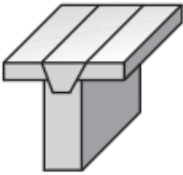
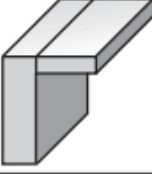
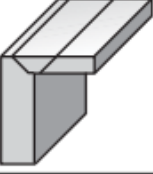


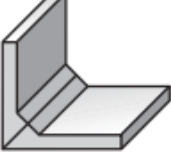
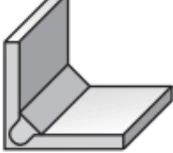


In comparison, the FSW process can achieve better strength, fewer voids and lower distortion after the weld is made, attaining results as shown in Figure 10, where the seam is more uniform and could have better superficial finishes compared to the arc welded counterparts because it does not require filler material as usually happens during fusion welding and the base metal does not liquify during process, leading to a better control of the seam region comparatively speaking.



**Figure 10.** Left images, MIG welds on aluminum. Right images, FSW process [28]

The usual weld configurations performed using FSW are listed in Table 1. Those looking for easy access for the tool, relatively simple fixtures, and parallel contact between the faces of the material used because finally those considerations limit the implementation of the process.

**Table 1.** Usual joint configurations for FSW [22]

Joint design	Before welding	After welding
Combination of a lap joint and butt joint		
Butt joint		
Combination of a lap joint and butt joint		
T-joint		
Corner joint		
Lap joint		
Corner joint		
Butt joint		

## 4.4 Regulation

There have been attempts from the European and American regulators, ISO and American Welding Society (AWS) respectively, to draft general requirements needed for the acceptable of joints aiming for industrial requirements.

The European framework approved in June 2011 by the name “Friction stir welding — Aluminium (ISO 25239-1:2011)”, describes the general vocabulary, types of welded joints and all the related information with qualification and inspection. This document is meant to



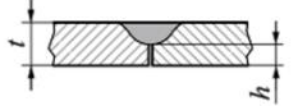
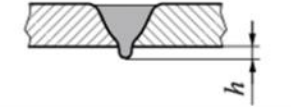
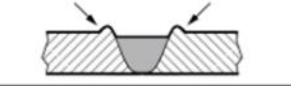
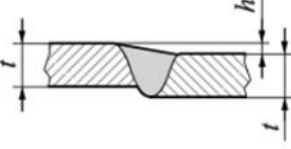
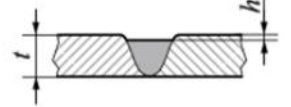
be applied all around the European Union and was design primarily for aluminum alloys and valid to diverse industries such as railway, aerospace, marine and food processing [24], [37]–[40]. The requirements needed for a successful weld, using tensile tests, are presented in Table 2, Table 3 and Table 4.

**Table 2.** ISO requirements [40]

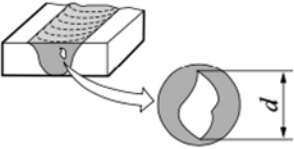
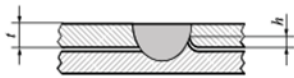
Material type	Temper condition of parent material before welding <sup>a,b</sup>	Postweld condition	Joint efficiency factor $f_e$
Pure aluminium	All temper conditions	As welded	1,0 <sup>d</sup>
Non-heat-treatable alloys	All temper conditions	As welded	1,0 <sup>d</sup>
Heat-treatable alloys	T4	Natural ageing <sup>c</sup>	0,7
	T4	Artificial ageing <sup>c</sup>	0,7 <sup>e</sup>
	T5 and T6	Natural ageing <sup>c</sup>	0,6
	T5 and T6	Artificial ageing <sup>c</sup>	0,7 <sup>e</sup>

<sup>a</sup> Refer to ISO 2107.  
<sup>b</sup> For parent material in tempers not shown,  $\sigma_{\min,w}$  shall be in accordance with the design specification.  
<sup>c</sup> Ageing conditions shall be in accordance with the design specification.  
<sup>d</sup> Irrespective of the actual parent material temper used for the test,  $\sigma_{\min,pm}$  is based on the specified minimum tensile strength of the "O" condition.  
<sup>e</sup> Higher properties can be achieved if a full postweld heat treatment is applied;  $\sigma_{\min,w}$  shall be in accordance with the design specification.

**Table 3.** Defects and acceptance [40]

Designation of imperfection	Remarks	Testing and examination in ISO 25239-4 <sup>a</sup>	Acceptance levels <sup>a</sup>	Reference number in ISO 6520-1 <sup>[3]</sup>
<b>Surface imperfections</b>				
Incomplete penetration		ME	Not permitted	— <sup>c</sup>
Excess penetration		VT, ME	$h \leq 3 \text{ mm}$	504
Toe flash		VT, ME	— <sup>b</sup>	— <sup>c</sup>
Linear misalignment		VT, ME	$h \leq 0,2t \text{ or } 2 \text{ mm, whichever is less}$	507
Underfill		VT, ME	$h \leq 0,2 \text{ mm} + 0,1t$ for $t \geq 2 \text{ mm}$ : $h \leq 0,15t$ for $t < 2 \text{ mm}$	— <sup>c</sup>
Irregular width	Excessive variation in width of the weld	VT	— <sup>b</sup>	513
Irregular surface	Excessive surface roughness	VT	— <sup>b</sup>	514

**Table 4.** Defects and acceptance (continued) [40]

Designation of imperfection	Remarks	Testing and examination in ISO 25239-4 <sup>a</sup>	Acceptance levels <sup>a</sup>	Reference number in ISO 6520-1 <sup>[3]</sup>
<b>Internal imperfections</b>				
Cavity		ME	$d \leq 0,2s$ or 4 mm, whichever is less	200
Hook		ME	— <sup>b</sup>	— <sup>c</sup>
<p><b>Symbols and abbreviated terms</b></p> <p><i>d</i> maximum transverse cross-sectional dimension of cavity (mm)</p> <p><i>h</i> height of an imperfection (mm)</p> <p><i>s</i> nominal butt weld thickness (penetration) (mm)</p> <p><i>t</i> nominal thickness of the parent material (mm)</p> <p>ME macroscopic examination</p> <p>VT visual testing</p> <p><sup>a</sup> When required, non-destructive testing should be carried out in accordance with ISO 3452-1 (penetrant inspection), ISO 17636 (radiographic testing) and ISO 17640 (ultrasonic examination). Testing and examination of other imperfections and their acceptance levels shall be in accordance with the relevant requirements or the design specification.</p> <p><sup>b</sup> Acceptance levels shall be within the specified limit of the relevant requirements or the design specification.</p> <p><sup>c</sup> See ISO 25239-1.</p>				

The American framework for FSW “AWS D.17.3 - Specification for Friction Stir Welding of Aluminum Alloys for Aerospace Hardware”, is focused on aerospace hardware and related components rather than the approach of the Europeans; following previous works done with welded specifications and commercial components grouped in the AWS D.17 standard. Since 2010 it has been valid, and the requirements needed for a sound weld are expressed in the Table 5.

Both standards have similar requirements for joint efficiency, minimum 70% to all heat treated aluminums and a minimum of 60% to those natural aged alloys [25] [38]. In general terms, there is agreement on the minimum mechanical limits that any joint must have. and must be completed with a visual inspection using the criteria presented in Table 5 and Table 6.

**Table 5.** AWS requirements for FSW [25]

Material Type	Temper Condition of Base Metal before Welding <sup>b</sup>	Postweld Condition <sup>c</sup>	Joint Efficiency Factor <sup>d,e</sup>
Pure aluminum	All tempers	As welded	1.0 <sup>f</sup>
Non heat treatable	All tempers	As welded	1.0 <sup>f</sup>
Heat treatable alloys <sup>g</sup>	T4	Natural aging	0.7
	T4	Artificial aging	0.7 <sup>h</sup>
	T5 and T6	Natural aging	0.6
	T5 and T6	Artificial aging	0.7 <sup>h</sup>

<sup>a</sup> The data in this table was taken from fusion welding specifications because no A-basis friction stir weld data were available.

<sup>b</sup> For base metal in other tempers not shown in this table, the ultimate tensile strength of the welded test specimen shall be in accordance with the Referencing Document.

<sup>c</sup> Aging conditions shall be in accordance with the Referencing Document.

<sup>d</sup> Joint efficiency factor = ultimate tensile strength of the welded test specimen after all postweld heat treatments have been conducted divided by the specified minimum tensile strength of the parent material required in the relevant specification.

<sup>e</sup> For combinations between different alloys, the lowest individual efficiency factor shall be achieved.

<sup>f</sup> The ultimate tensile strength of the base metal is based on the specified minimum ultimate tensile strength of the "O" (annealed) condition, irrespective of the actual base metal temper used for the test.

<sup>g</sup> Only applies to 6000 series alloys. For 2000 series and 7000 series alloys, the temper base metal before welding and the postweld aging conditions shall be in accordance with the Referencing Document.

<sup>h</sup> Higher properties may be achieved, if a full postweld heat treatment is applied. The ultimate tensile strength of the welded test specimen shall be in accordance with the Referencing Document.

**Table 6.** AWS acceptance criteria [41].

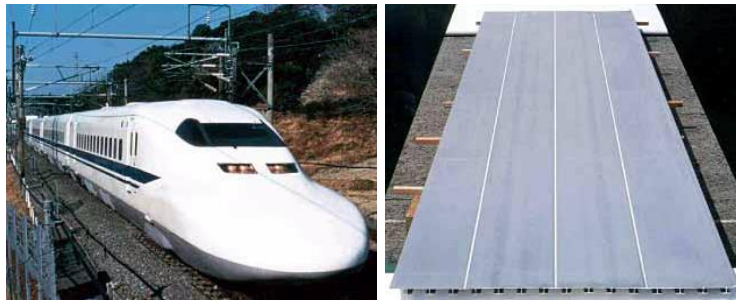
<b>Table 9.1</b>			
<b>Acceptance Criteria<sup>a</sup></b>			
Discontinuity	Class A	Class B	Class C
<b>Cracks</b>	None	None	None
<b>Incomplete joint penetration<sup>b</sup></b>	None	None	None
<b>Inclusions</b>			
a. Individual size (maximum)	.33T or 0.06 in [1.5 mm], whichever is less	0.50T or 0.09 in [2.3 mm], whichever is less	Not applicable
b. Spacing (minimum)	Four times the size of the larger adjacent discontinuity	Two times the size of the larger adjacent discontinuity	Not applicable
c. Accumulated length in any 3 in [76 mm] of weld (maximum)	1.33T or 0.24 in [6.1 mm], whichever is less	1.33T or 0.24 in [6.1 mm], whichever is less	Not applicable
<b>Internal cavity, or cavity open to surface</b>	None	None	Reject only cavities open to the surface
<b>Linear mismatch across joint (maximum)</b>	1.05 times the base metal thickness tolerance	1.075 times the base metal thickness tolerance	Not applicable
Groove welds only			
<b>Overlap (cold lap)</b>	See 8.6	See 8.6	See 8.6
<b>Angular distortion (degrees) (maximum)</b>	3 degrees	3 degrees	Not applicable
Groove welds only			
<b>Underfill (maximum)</b>			
Applies only if the weld face will not be postweld machined			
a. For the full length of the weld (maximum depth)	0.05T	0.075T	0.10T
b. Individual defect (maximum depth)	0.07T or 0.03 in [0.76 mm], whichever is less	0.10T or 0.03 in [0.76 mm], whichever is less	0.125T or 0.03 in [0.76 mm], whichever is less
c. Accumulated length in any 3 in of weld (maximum)	0.20 in [5.1 mm]	0.60 in [15 mm]	1.0 in [25 mm]
<b>Weld flash (maximum height)</b>	See 8.6	See 8.6	See 8.6

<sup>a</sup> See 9.4.1 for general rules regarding the acceptance criteria.

<sup>b</sup> Acceptance criteria of incomplete joint penetration does not apply to partial joint penetration welds.

## 4.5 Industrial Background

There have been successful attempts for joining aluminum and other lightweight materials around the globe using FSW in the railway industry [42], keeping dimensional accuracy and mechanical properties. Examples of those applications are the wagons of the Shinkansen in Japan (Figure 11), where the ceiling was built using sheets of aluminum joined by this process [43].



**Figure 11.** Japanese bullet train made by FSW [43]

Followed by Hitachi's first viable economic implementation of FSW, joining wagons and comparing the results with GMAW welding, sorted in the trains observables in Figure 12.



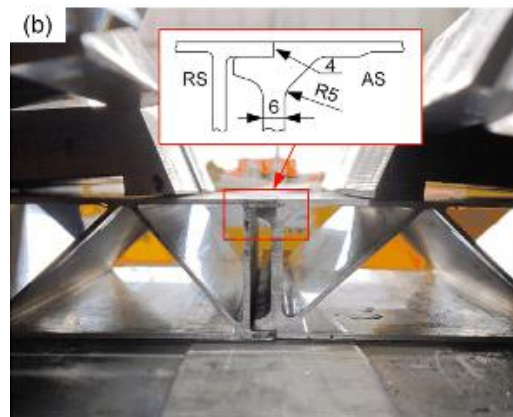
**Figure 12.** HITACHI trains using FSW [44].

In Europe, Sapa and Hydro Marine were the first to use it commercially on the fabrication of side panels of their wagons. Particularly since 1997 [21][43], the German manufacturer Alstom LHB has been building pieces which are acquired by European assemblies to construct trains like the one shown in Figure 13 [45]; and in 1999 achieving feasible and economically viable joints of aluminum thicker than 17 mm and cheaper compared with other arc methods.



**Figure 13.** Alstom LHB trains made using FSW [45]

All of this is confirmed by authors like Xiangqian *et al* [46], who reported on the feasibility of welding hollow profiles of AA6005 – T6 using dedicated FSW machinery (Mega Stir) in a butt joint configuration as shown in Figure 14, implementing a traditional tool with an inclination between 1 to 3 degrees. It is important to notice that this machine is set to perform welds using force control instead of position. They finally report efficiencies against base material of around 78%.



**Figure 14.** Configuration of weld [46]

One advantage discussed in the article “*Application of Friction Stir Welding to Construction of Railway Vehicles*” and not greatly talked about is focused on the necessity of less skilled welders to perform the joints using FSW compared with GTAW (Gas Metal Arc Welding), leading to lower costs and less dependence on know-how workers [47]. Also, as the welds were tested, it was concluded that it is possible to obtain seams with 98% of efficiency to the base metal.

As mentioned before, tools directly influence the correct parameter selection, but the information available for railway applications is scarce. Some of the authors that referred to this are Huang *et al.* performing welds with a bobbing tool (Figure 15), which does not require a backing plate and achieved efficiencies greater than 86% compared with the base metal (AA6005) [48].



**Figure 15.** Bobbing tool for extruded profiles [48]

In Colombia, after a review of different authors the FSW process started to be studied in 2008 using available conventional machinery, as reported by Franco *et al* [14], where a milling machine was paired with basic FSW tooling. Successful results were obtained and lead to development in consequent years.

Later on, the study focused on the evaluation of different aluminum alloys from the series 1000, 2000, 6000 and 7000; magnesium alloys and some superficial enhancements of steels. Trying to broaden the knowledge of welding method, compared against the local material availability and fulfilling the difficulties of arc joining techniques. For this, parameter development has been crucial for identifying the best welding conditions to obtain sound welds, broadening the locally acquired knowledge [49][50][16][51]. In the last approaches, phenomena as residual stresses, tool analysis and numerical models have been proposed in order to understand better the material flow with the local limitations [17][15][52].

Nevertheless, all this local development has only been done from an academic perspective because the industry remains largely unfamiliar with the process despite the successful developments done locally and the possibility of implementation with local conventional machinery.

## 5. Methodology

This work aims for the development of a manufacturing procedure using Friction Stir Welding (FSW) on a component from Metro de Medellín's MAN trains. In the following paragraphs are the steps followed to obtain these results, also presented in schematic form in Figure 16.

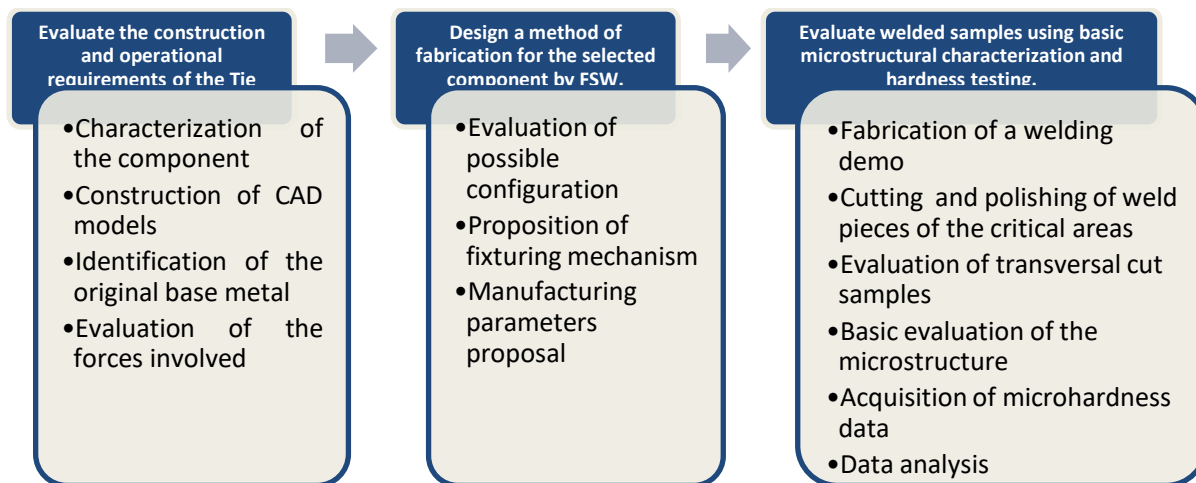


Figure 16. Methodology proposed.

### 5.1 Specific objective 1 goals

#### *Evaluate the construction and operational requirements of the tie.*

1. Characterization of the component:

Involves the assessment of materials used in the manufacturing of the Tie, and geometrical features which could be constructed using FSW. Finally identifying the assembled components for further analysis.



## 2. Construction of CAD models:

Using the original parts involved in the mechanism, digital modelling was made using the commercial software *Inventor Pro* and *Fusion 360* with their respective academic licenses before any mechanical evaluation.

## 3. Identification of the original base metal:

Using the principle of optical emission spectrometry, where an electric current excites the atoms of the sample until it evaporates and a specific wavelength light is emitted to be later compared with the pure element data to obtain a map of constituents of the sample [53]. A sample of the piece was evaluated to identify the original alloy metal using a BRUKER Q8 MAGELLAN spectrometer at 23.5°C and 25% of relative humidity.

## 4. Evaluation of the forces involved:

For the mechanical evaluation of the component a free body diagram was constructed, complemented with a finite element analysis (FEA) using the *Inventor Pro* software, to assess the maximum stress and loading paths experimented by the component during operation.

## 5.2 Specific objective 2 goals

### *Design a method of fabrication for the selected component by FSW.*

#### 1. Evaluation of available materials and configurations:

After assessing the component, a further material consideration was held aiming to select a proper replacement of the alloy previously identified for local manufacturing, taking into consideration its availability and geometry to fulfil the geometrical requirements.

#### 2. Proposition of a fixturing mechanism:

In accordance with the geometrical modifications of the component evaluated and selected, a fixturing mechanism was proposed to implement FSW locally, taking into consideration the available machinery for further construction, fulfilling the mechanical requirements of the piece.

### 3. Manufacturing parameters proposal:

Having all the information around the component and available material, a selection of parameters adequate for the alloy and configuration proposed was selected for its construction. This will address the tooling, rotational and translational setup and other requirements to carry on the welding process, this step was nourished with the experience of TWI in relationship with the FSW process.

## 5.3 Specific objective 3 goals

*Evaluate welded samples using basic microstructural characterization and hardness testing.*

Finally, for this objective is proposed:

1. Fabrication of a welding demo component using the data acquired.
2. Cutting of welded sections of the critical areas to be polished by emery paper from 400 to 3000 grit, followed by diamond polish.
3. Evaluation of samples, considering the possible discontinuities present in a FSW weld.
4. Basic evaluation of the microstructure and transversal cut of the weld sample after being attacked by Keller reagent.
5. Acquisition of micro hardness data of the weld pieces using an *Indenter ZHμ* machine against the base metal to compare its properties.

After the microstructural analysis, the acquisition of micro harness data was performed using an *Indenter ZHμ* machine coupled with a Vickers' head set up to 300 g force for 10 seconds. Drawing a line from the top of the weld at 300 μm and testing every 1 mm horizontally, additionally, a vertical line will be drawn, and data acquired every 0.5 mm in the middle of the seam.

### 6. Analysis of the data

Finally, with all the information acquired, an evaluation of the proposed welds was made. Additionally, the project was accompanied by:

## **5.4 Bibliographical research**

For the whole project, bibliographical research was made using the University's databases, additionally supported by blueprints and relevant information of the selected component obtained in the warehouse of the Metro de Medellín. All of this backed by engineers and expert's knowledge.

## **5.5 Results**

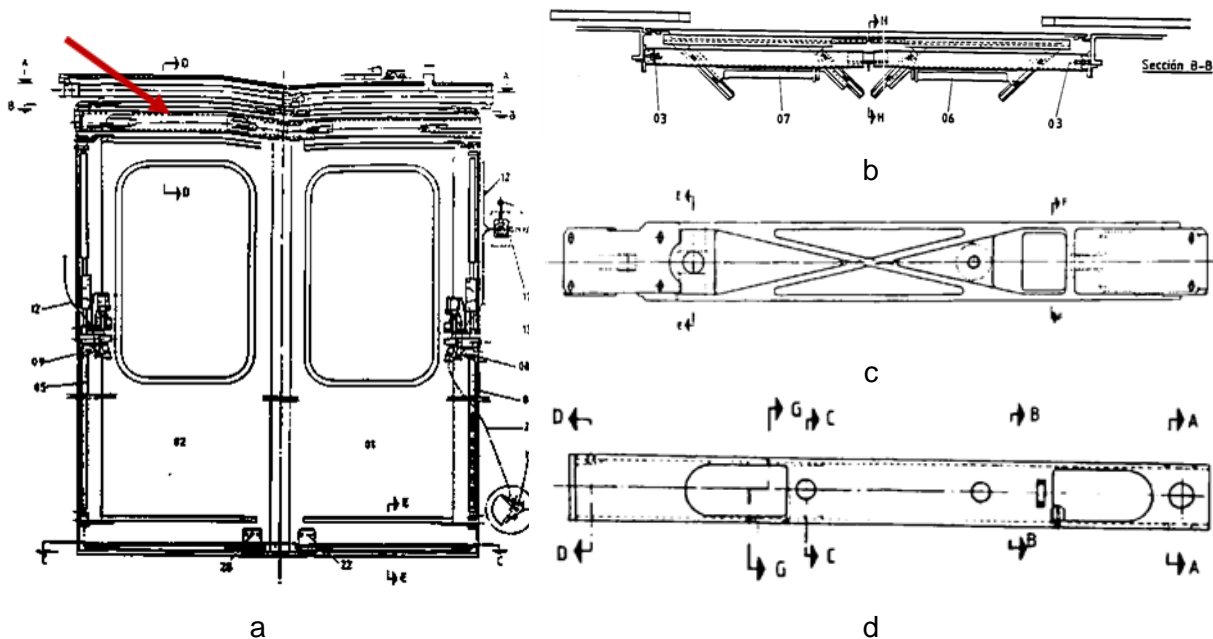
With the data collected, a structured welding procedure was proposed for the evaluated component, appropriate for the local industry in order to obtain successful welds with the aluminum family identified, helping to broaden the knowledge related to the FSW process in the regional industry and fulfilling the growing demand of railway components with the metal mechanic sector.

## 6.Results

### 6.1 Construction and operational requirements for the tie

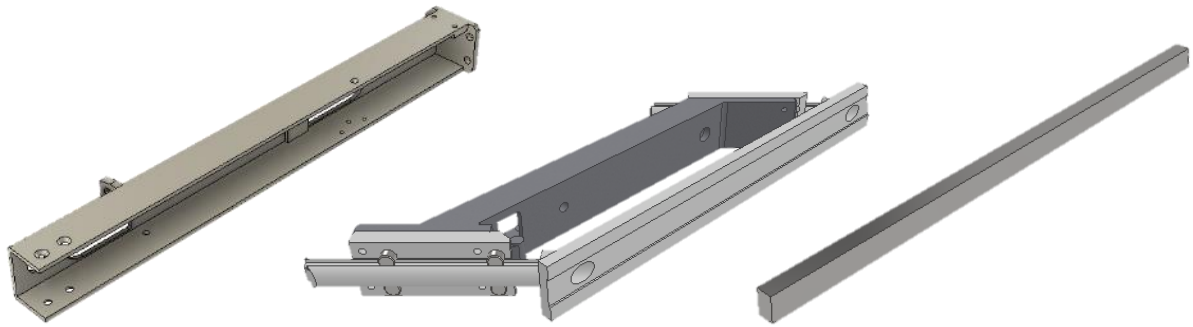
#### 6.1.1 Tie's description

The ties are located on the upper flange of every door of the MAN wagons (Figure 17 – a) and coupled with other modules to build up the mechanism which allows the movements of the door. Figure 18 shows the rail, tie, and support body of the assembly in a more detailed perspective. And Figure 19 indicates the position of the mechanism when the door is closed and open.



**Figure 17.** Tie's location, a) door assembly, b) mechanism assembly, c) mobile mechanism backbone and d) tie.

The tie's role is to link the mechanism shown in Figure 18 – b with the frame of the wagon, thus supporting the doors and their movement as the structural member of the assembly.



**Figure 18.** Mechanism assembly, from left to right: Tie, Support body and rail



**Figure 19.** Displacement of the components. a) assembly when the door is closed, b) assembly when the door is open

For the past decade, the loading of this component has changed significantly because the Aburra's Valley population has increased rapidly, greater than the 6,5% projected growth for the country (approximately at a rate of 12.34%) [54]. This increase has affected MdM because required the adjustment of its train frequency in a proportional manner with the demand, translated into more cycles per day for this part.

To have an idea of the number of cycles that the component withstands, the longest service line (line A) has 20 train stations, which equals 20 opening and closing movements per journey coupled with 7 cycles per day, raising the count to near 280 runs. Making the same analysis for the B line (the shortest track), each door opens approximately 252 times a day. To finally get cycle values to range between 92 and 102 thousand cycles per year depending of the Metro route.

### 6.1.2 Maintenance records

At MdM's maintenance department, the different components of the wagons are classified into two main categories:

1. Equipment: those elements needed for a daily operation like the electric motors, compressors, gear components, etc. This category has better and more controlled maintenance guidance since those parts guaranty continuous operation.
2. Supplies: related to all the consumables used as replacement parts during inspections. In this group are classified the bearings, seals, bulbs, etc.

The ties are classified as supplies, reflecting the scarcity of information regarding their maintenance, usage and replacement. However, there are some data related to the number of repairs and maintenance orders as is shown in Table 7.

**Table 7.** Tie maintenance data.

<b>Component</b>	<b>Number of repairs</b>	<b>First maintenance</b>	<b>First new component change</b>	<b>Number of new components manufactured</b>
Left design	107	12/05/2006	3/07/2012	19
Right design	57			16

Different local manufacturers have provided new components over the years to supply the company with spare parts, and back in 2010, the company performed a technical evaluation to obtain blueprints to guaranty the quality and functionality of these elements. Some of the locals that have constructed ties are *Industrias REYMO, Maquinados e Hidráulicos, Metal Works and EDAFA*.

The first manufacturing attempt was made in partnership with the local company EDAFA using the information structured in the archive OTT 130 (Annex 1) from Metro's data library. It is important to note that the company does not perform any evaluation of the materials used, trusting in the good faith of the locals.

With the information obtained, it is possible to say that the original pieces had a lifespan of about 11 years (since 1995).

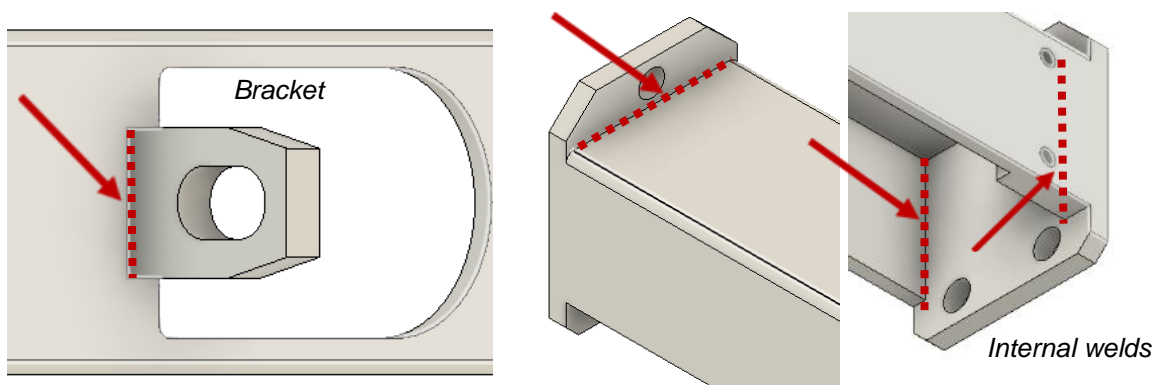
### 6.1.3 General geometry

There are two types of ties used in the door mechanism, the first made by the original manufacturer and the second from local suppliers as shown in Figure 20. Comparing them, it is observable a thickness change only in the locally manufactured components to enhance their mechanical performance (Figure 20).



**Figure 20.** CAD models of the ties. At left the original, at right the locally manufactured. On the side a zoom of the differences at the ties.

As mentioned, both are arc welded at the locations identified in Figure 21 (dotted lines), around the side base of the bracket and inside the perpendicular face which has the mounting holes.



**Figure 21.** Original weld locations.

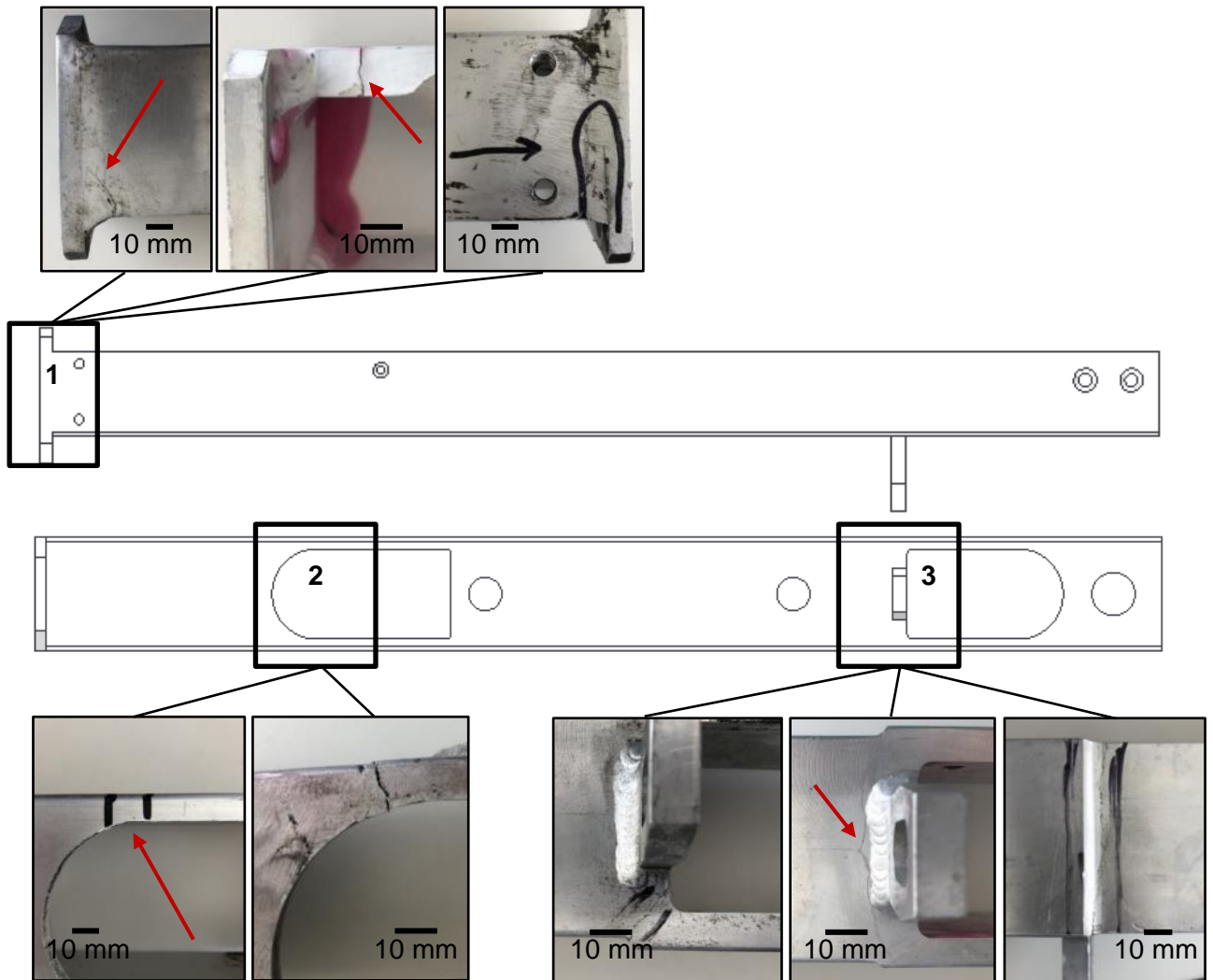
#### **6.1.4 Discontinuities and assessment**

A visual inspection was made to various ties to identify the most common discontinuities and results are summarized in Figure 22. Starting from the left side of the image it is possible to observe cracks with a length of 10 mm (or more), which are located not in the weld itself but over the heat-affected zone (marked in zone number 1). Those discontinuities pass through the thickness of the “C” profile and in some cases on both sides.

Another type of discontinuity is observable around the number 2 zone, possibly a product of continuous stresses due to the opening and closing movements. Usually, this discontinuity starts from the inner side of the hole and continues all the way through the wall of the profile. Finally, in number 3, around the base of the bracket, some cracks appear on the edge of the perforation and continue around the heat affected zone left by the arc weld or even travelling across a stress concentration geometry as presented.

All discontinuities show the same pattern, starting from an edge and continuing around a heat affected zone or a stress concentration area until reaching around 10 mm when the piece is either repaired or replaced.

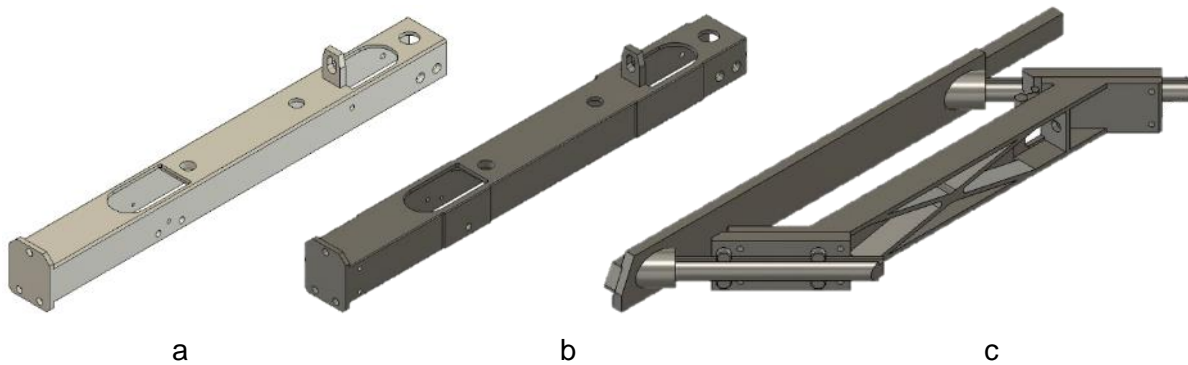




**Figure 22.** Presence of discontinuities around the tie

### 6.1.5 CAD models

With the usage of *Inventor Pro* and *Fusion 360* as commercial software, CAD models were constructed (as presented in Figure 23), following the geometric characteristics of the components.



**Figure 23.** Images of CAD models, a) Original Tie, b) Locally made Tie and c) Door mechanism.

### 6.1.6 Identification of the base metal

The results obtained from chemical analysis of the original ties, using a Bruker Q8 Magellan optical spectrometry equipment at 23.5°C and 25% of relative humidity are detailed in Table 8. Those outcomes indicate a high percentage of Magnesium and Silica, which are an indicator of an aluminum alloy from the 6XXX series [55].

**Table 8.** Chemical composition of the original ties

Element	%/w	Element	%/w
Silicon (Si)	0.4860	Calcium (Ca)	0.0035
Iron (Fe)	0.2190	Cobalt (Co)	<0.0010
Copper (Cu)	0.0560	Phosphorus (P)	0.0008
Manganese (Mn)	0.0140	Lead (Pb)	0.0012
Magnesium (Mg)	0.4950	Tin (Sn)	0.0040
Chrome (Cr)	0.0015	Vanadium (V)	0.0053
Nickel (Ni)	0.0031	Zirconium (Zr)	0.0013
Zinc (Zn)	0.0051	Antimony (Sb)	0.0016
Titanium (Ti)	0.0120	Arsenic (As)	0.0035
Boron (Br)	0.0008	Aluminum (Al)	98.69

After further scrutiny, to obtain a specific and suitable alloy with the chemical composition, four different possibilities were identified: AA6005, AA6060, AA6063 and AA6101

[56][57][58][59]. Each material was reviewed and the most likely material for this railway application is the AA6063, because:

- It has good mechanical performance, suitable for a similar application compared with the other aluminum alloys.
- It was available as a heat-treated alloy to enhance its mechanical properties.
- It has been used for extrusion components (as the tie) and in machined applications.
- Has excellent corrosion resistance.

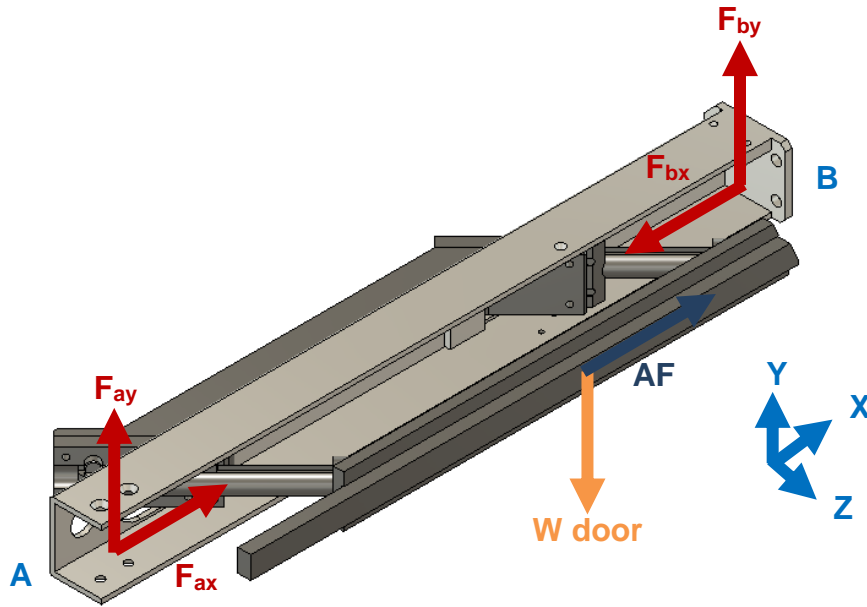
Additionally, it has been reported to be used in the railway industry since it is suitable for intricate geometries made by extrusion [60].

### 6.1.7 Free body diagram

Before performing the FEA, an analytical evaluation was carried out to corroborate the results, giving ground to accept the simplifications implemented in the commercial software. The free force diagram shown in Figure 25 was based on the mechanism distribution and operation of the real components (Figure 24) and corroborated with the schematics shown in Figure 17. The mechanism has two critical states, the first one is when the door is completely closed and the second one, when it is open; with a 22.45 and 78.4 mm of moment arm respectively considering the door's center of mass.



**Figure 24.** Component selected – tie



**Figure 25.** Free body diagram

Were:

- $F_{ax}$  and  $F_{bx}$  are the components in the X-axis, corresponds to motion restrictions.
- $F_{ay}$  and  $F_{by}$  are the components in the Y-axis, corresponds to motion restrictions.
- $W_{door}$  is the weight of the door, 35 kg.
- $AF$  is the pneumatic actuator force, 2800 N at 5 Bars

The equations, which describes the statics of the assembly, are:

$$(1) \Sigma F_x : F_{ax} + F_{bx} + FA = 0$$

$$(2) \Sigma M_A : W_{door}(0.52 \text{ m}) - F_{by}(0.78 \text{ m}) = 0$$

$$(3) \Sigma F_y : F_{ay} + F_{by} - W_{door} = 0$$

$$(4) F_{ax} = F_{bx}$$

Having as result the forces with their corresponding value as shown:

$$F_{ax} = 1400 \text{ N}$$

$$F_{bx} = 1400 \text{ N}$$

$$F_{ay} = 114.45 \text{ N}$$

$$F_{by} = 228.9 \text{ N}$$

$$W_{door} = 343.35 \text{ N}$$

The free force diagram were used in the stress evaluation of the component using the formulas presented below [61]:

For the torsional values

$$(5) M_{ti} = \frac{a_i^3 b_i}{\sum_{i=1}^n a_i^3 b_i} M_t$$

$$(7) \delta = \frac{3M_t}{G \sum_{i=1}^n a_i^3 b_i}$$

$$(8) \tau_{max_i} = \frac{3M_t a_i}{\sum_{i=1}^n a_i^3 b_i}$$

For the normal values

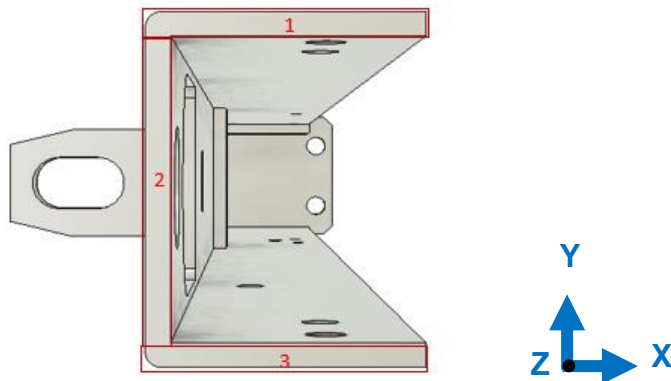
$$(6) \sigma = \frac{M_n c}{I}$$

For the shear values

$$(9) \tau = \frac{VQ}{It}$$

Were:

- $M_{ti}$  is the momentum of each subdivision (Figure 26) around the rotational Z axis.
- $\delta$  is the displacement of each subdivision.
- $\tau_{max_i}$  is the maximum shear value of each subdivision.
- $a_i$  is the shortest longitudinal dimension of each subdivision (Figure 26)
- $b_i$  is the longest longitudinal dimension of each subdivision (Figure 26)



**Figure 26.** Transversal subdivision

After all the calculations and applying the Von Mises analysis on a differential cube at the outer part of section 3 (because it presents the greater stresses) the results obtained are shown in Table 9.

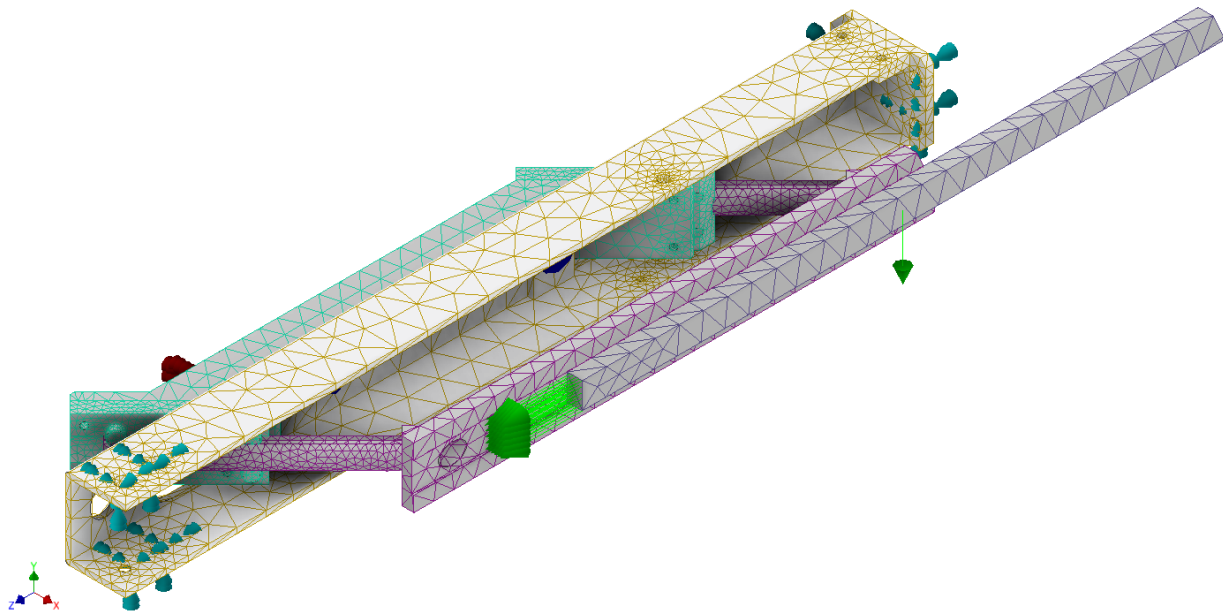
**Table 9.** Manual calculations

Orientation	Sigma 1	Sigma 2	Max stress (MPa)
XY	3,23	3,23	<b>3,23</b>
ZY	1,06	0,53	<b>0,91</b>
ZY	3,81	3,28	<b>3,57</b>

### 6.1.8 FEA analysis

For the computational simulation the software Autodesk *Inventor Pro* was used, with the following parameters applied to the CAD model:

- Door's weight: 35 kg
- Pneumatic actuator force at 5 Bars of pressure equivalent to 2800 N
- For the original ties, AA6063-T6 alloy, obtained by the chemical composition shown previously.
- For the new ties, AA 7075-T6 alloy was used.
- Bolted connections in the holes and constraints at the end of the component.
- Two simulation conditions, when the door is fully opened and closed (74,5 mm and 22,5 mm), which are the most critical situations.

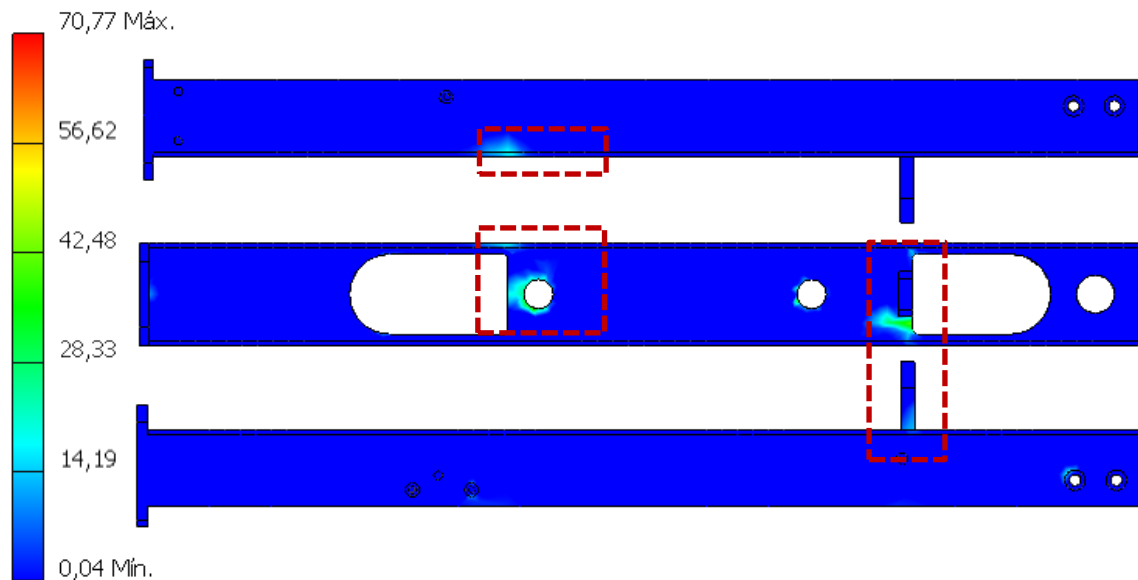


**Figure 27.** FEA constrains and considerations

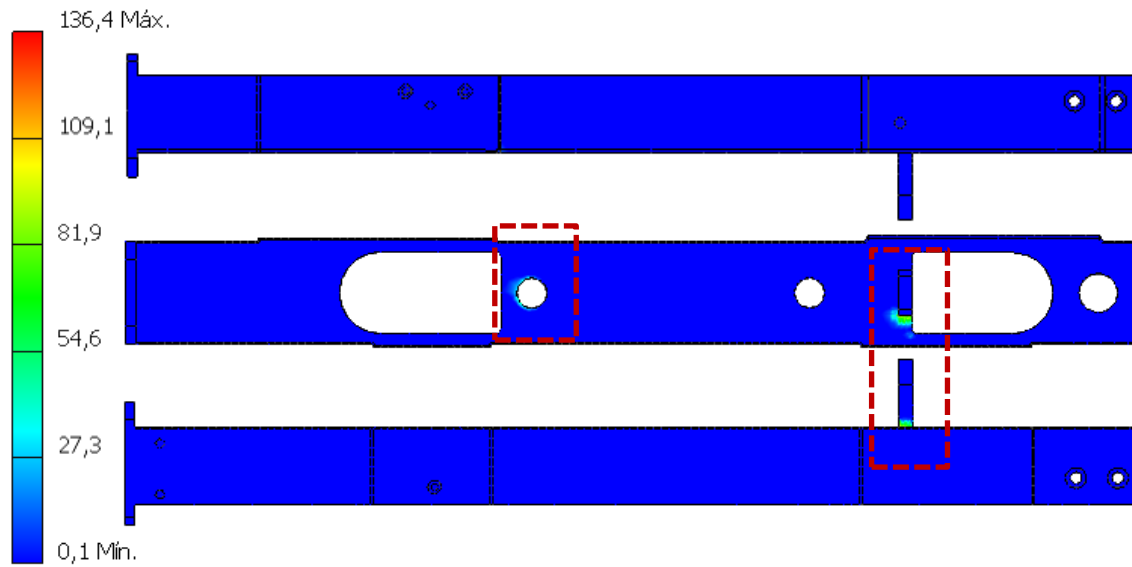
The mesh implemented and general dispositions in the analysis follow the conditions below to guarantee the best results and schematically presented in Figure 27, in accordance with the free force diagram:

- Convergence criteria were set to 5% of error in mesh size, applied to the Von Mises analysis to ensure the stresses because it is the strictest criteria.
- A tetrahedral finite element (FE) with curve faces was used to ensure the adaptation to the geometry at the edges, and a parabolic form function equation to complement this general form.
- A non-structured mesh, with adaptative capabilities around the higher stresses to guaranty the convergence.
- As heuristic conditions, a maximum of 30 degrees of change between FE, an upper limit of 1.5-dimensional difference between faces, and adaptative mesh around the edges of the bracket (Figure 21).

At first glance, the simulations made in the open condition have the same behavior as expected and identified in the ties, having the greatest stresses around the bracket and the perforations shown in Figure 28 and Figure 29. With maximum Von Mises values of 70,8 MPa and 136 MPa for the original and locally manufactured components respectively. Additionally, comparing the results with the data from Table 9 the results vary less than 1% (corresponding to 3.2 MPa 0.9 MPa and 3.54 MPa respectively), which makes acceptable the analysis for further computational evaluation.



**Figure 28.** Open mechanism - Original piece

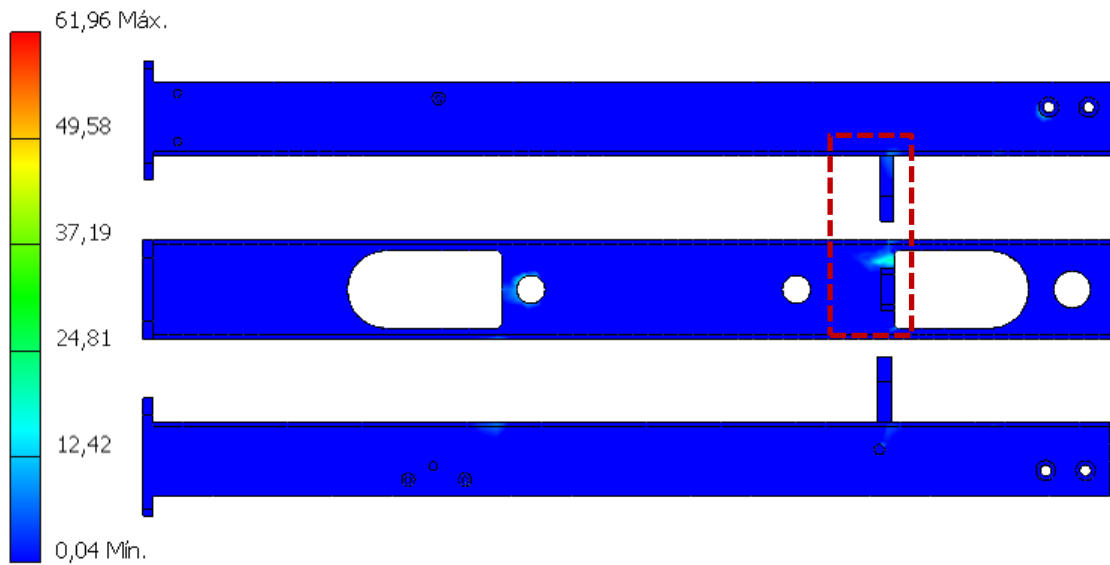


**Figure 29.** Open mechanism - locally manufactured

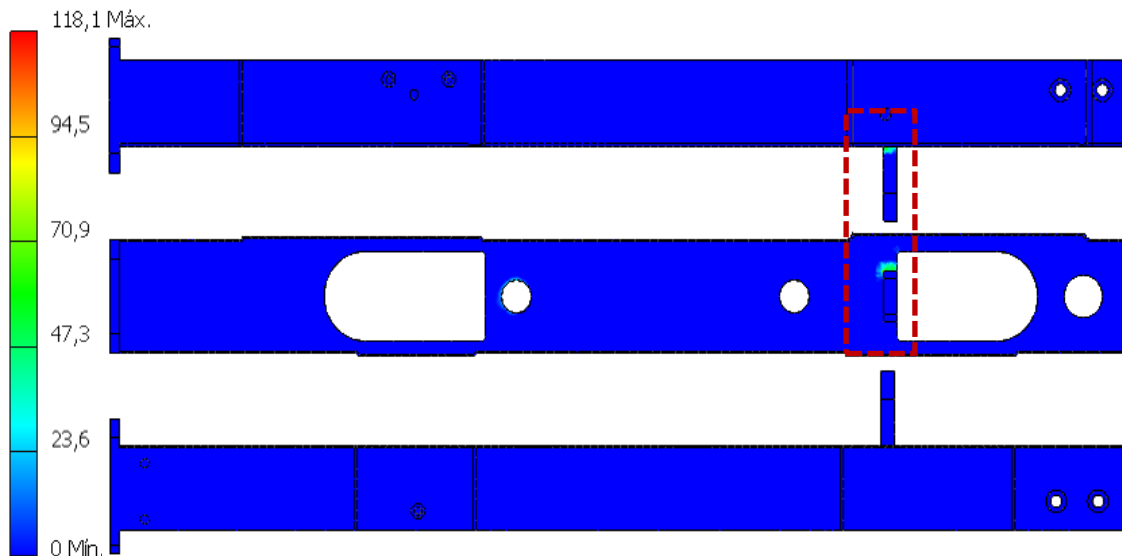
The same behavior is observable in the simulations made with the closed condition described before (Figure 30 and Figure 31). Comparing it to previous results, the maximum stresses are located on top of the bracket with values of 62,0 MPa and 118,1 MPa for the original and locally made components.

All this information helps to conclude that the most critical part of the Tie is the bracket, having the greatest stresses and cyclic loading, being critical from a fatigue standpoint and affecting the life expectancy of this piece.



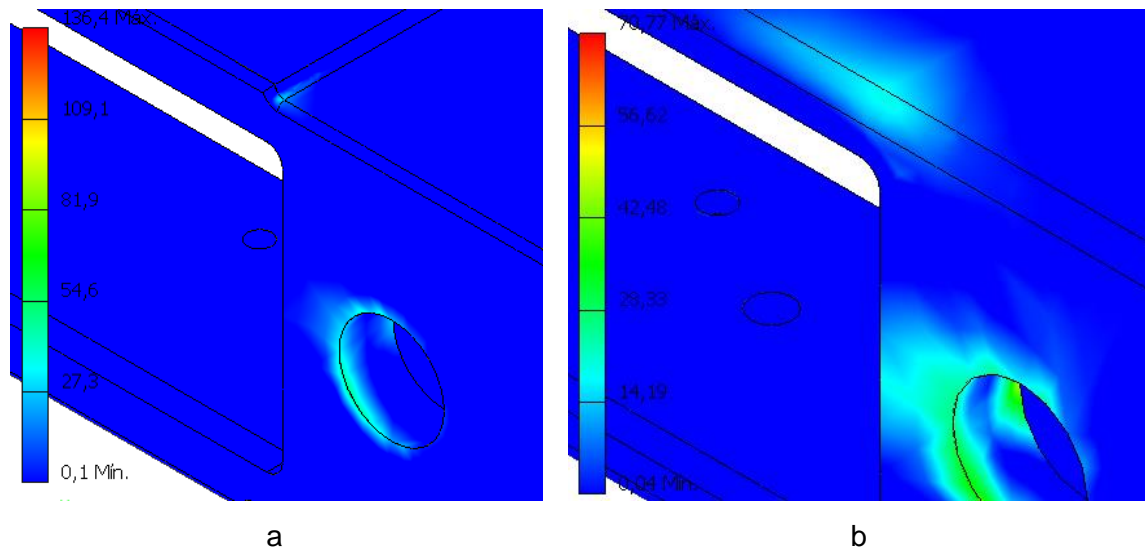


**Figure 30.** Closed mechanism – Original piece



**Figure 31.** Closed mechanism - locally manufactured

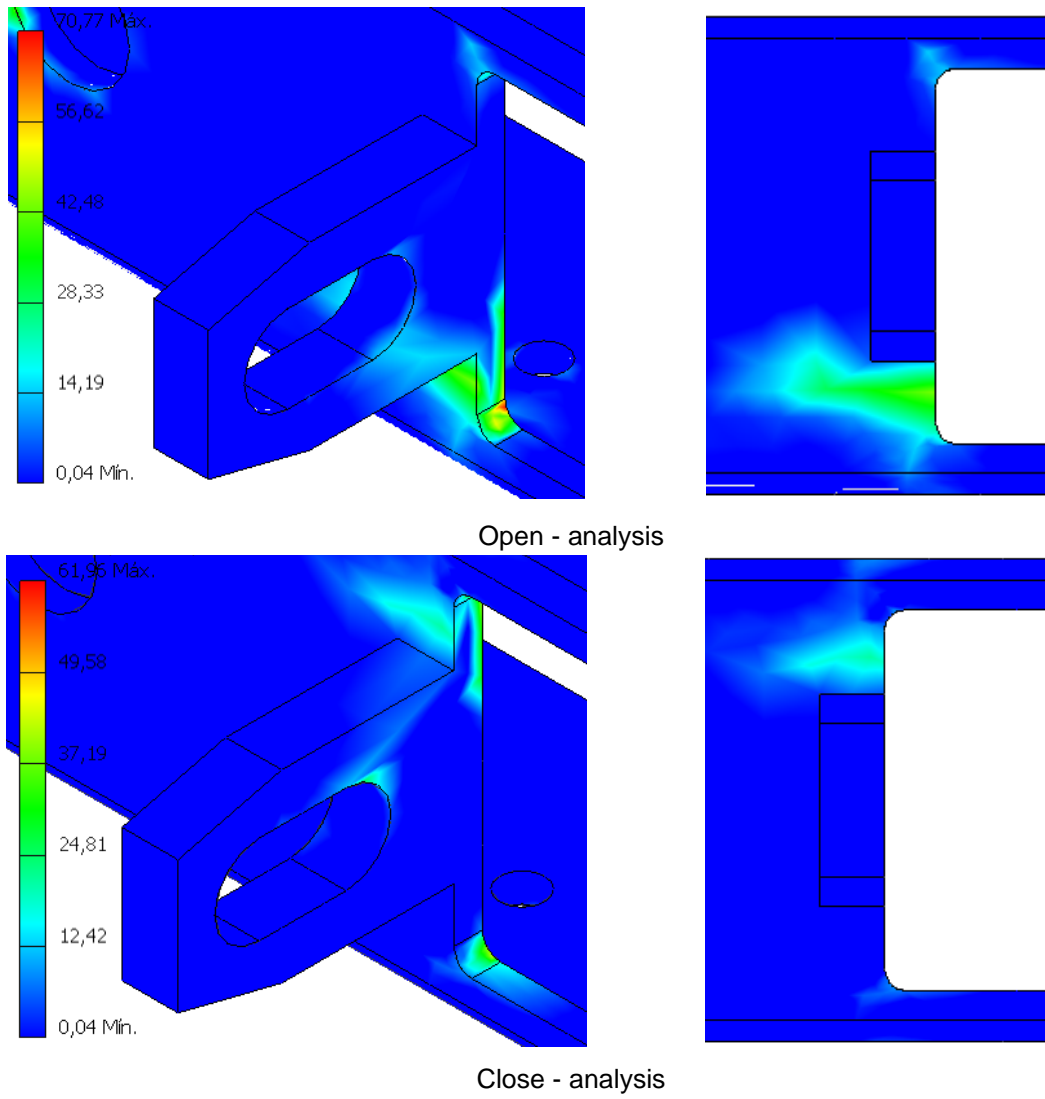
A deeper analysis of the stress distribution over the pieces shows that the locally made components have a stress concentration area at the section change, contrary to a more uniform distribution in the original tie geometry. These values vary from 48 – 51 MPa, against 25 – 29 MPa obtained in the original component (Figure 32). This thickening is not useful, only adds weight and a geometric discontinuity and suggesting that this feature is not relevant for addressing the discontinuities on the tie.



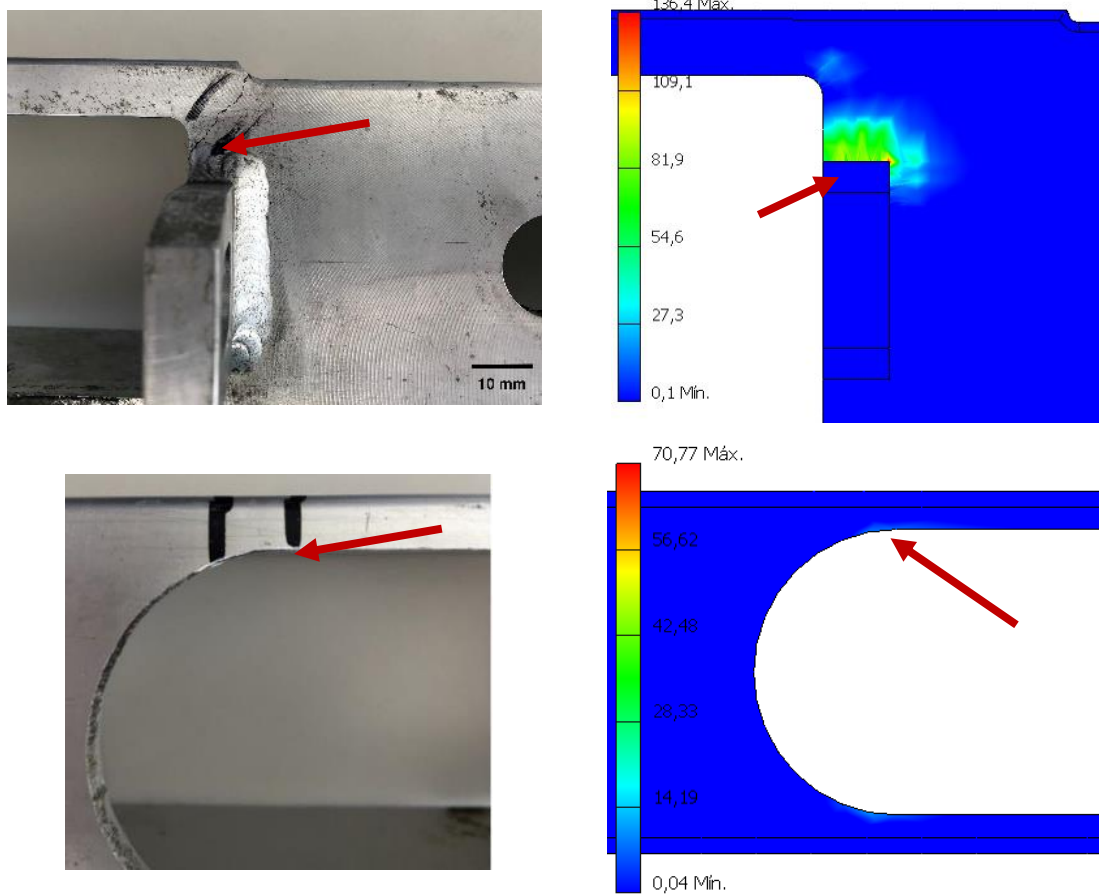
**Figure 32.** a) Locally made component, b) Original piece

At the Bracket (Figure 21), both simulations behave like the stress distribution on Figure 33, from an open or closed perspective with similar values of stress, between 30 MPa to 71 MPa with the peak values at the edges.

Compared with the appearance of cracks in the physical components, the zones with higher stresses are directly related to those defects like the images shown in Figure 34; but values of stress obtained in a static analysis do not surpass the limits of elastic deformation of the base metal (AA 6063- T6 = 214 MPa [62] and AA 7075 – T6 = 462 MPa [63]), and those discontinuities may be linked with fatigue failure and microstructural changes around the heat affected zone from the welds.



**Figure 33.** Bracket region stress

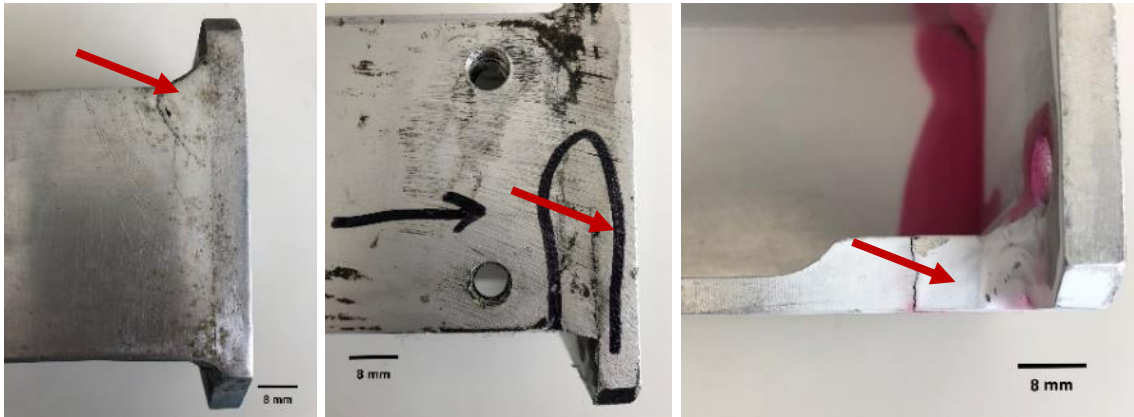


**Figure 34.** Cracks in the components related with stress.

Additionally, it was observed while inspecting different ties that some other cracks appeared next to the welds as shown in Figure 35, supporting the fatigue - heat affected zone hypothesis of failure.

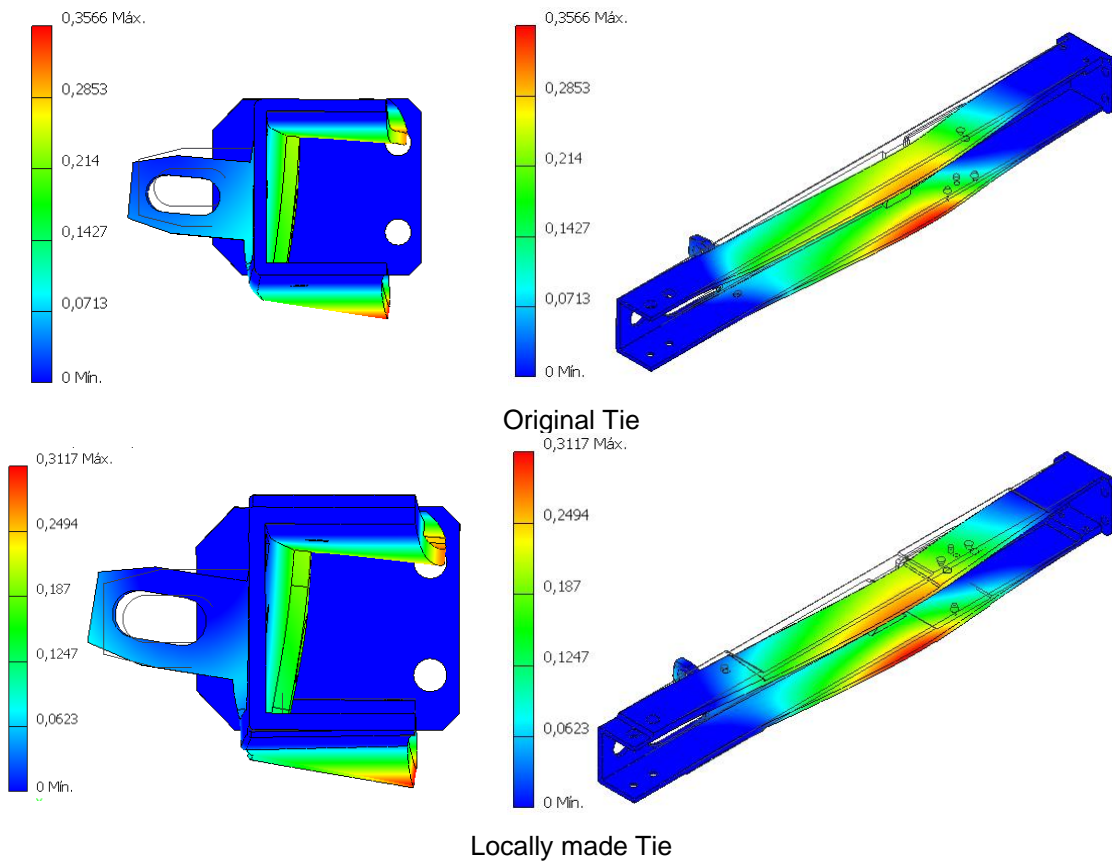
Literature related to this kind of discontinuities mentions that the appearance and propagation of cracks next to the heat-affected zone is a mechanism of failure that can be linked with many load cycles over the life span of the component (what happens in this component) or high stresses, in combination with a diminution of maximum yield strength of the material and geometrical characteristics [64], [65].

In this case, the information shared by Metro's warehouse identifies the initial failure of components was approximately after 15 years of continuous operation, but the data is not presented in a very accurate way and without any description of crack growth.



**Figure 35.** Heat affected zone discontinuities

Also, the deformation obtained by the applied loads makes the tie twist clockwise as shown in Figure 36, with a maximum displacement of 0,36 mm and 0,31 mm for the original and new geometry respectively, in accordance with the deformation expected with the usage of the tie.



**Figure 36.** Rotation from the ties

The convergence graphs are presented in Figure 37, confirming the assumptions made between the stress and displacements selected for the FEA.

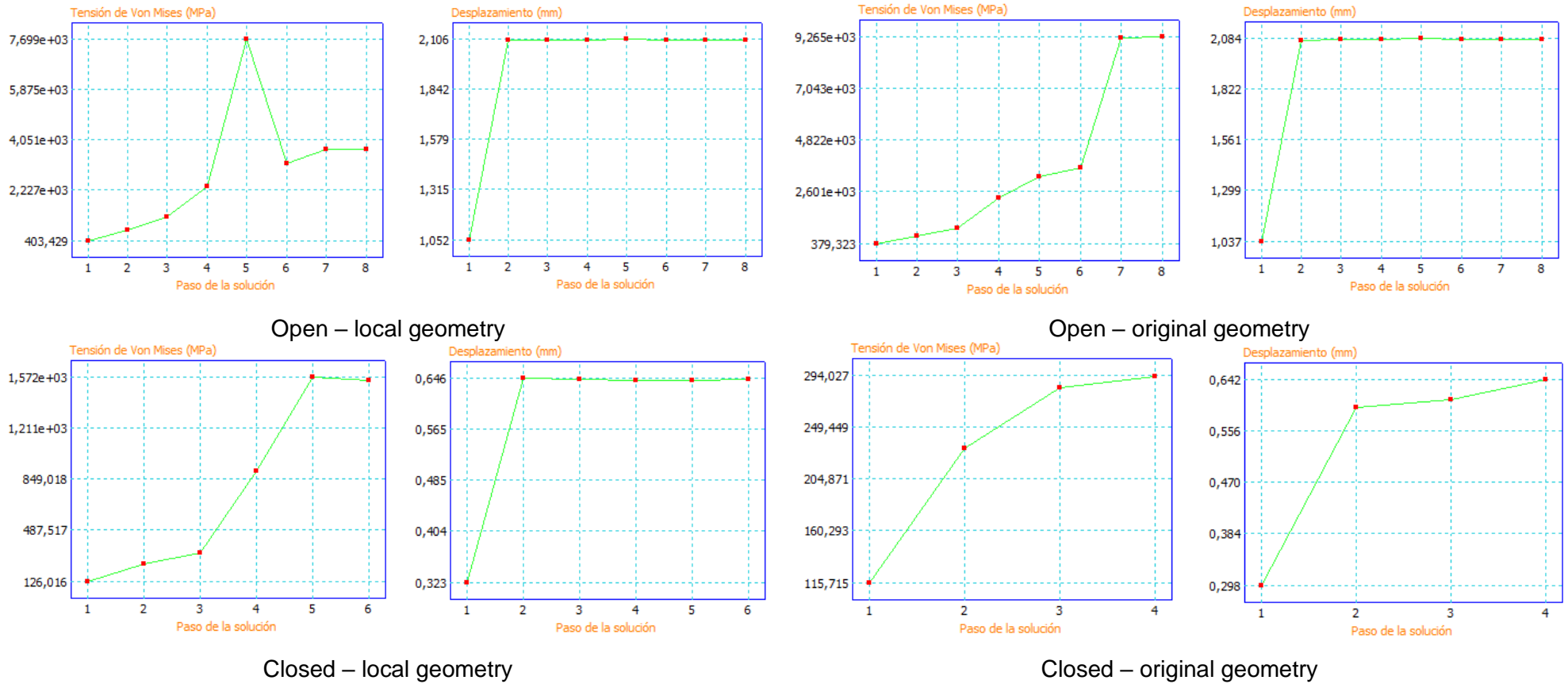
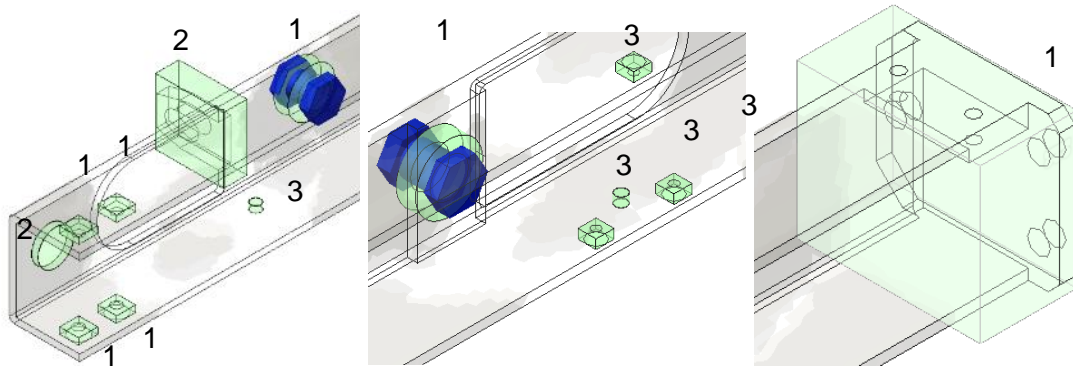


Figure 37. Convergence curves

### 6.1.9 Stress critical path

To obtain useful information to compare with the stress and displacement analysis and identify the load paths during operation for further modification to implement FSW, a topology optimization assessment was made. For this computation, the software *Fusion 360* from *Autodesk* was used with the same load and constraints characteristics as mentioned before.

As required by the study, some areas were geometrically constrained due to the physical connections needed at the wagons or for alignment at the assembly. Those can be identified in Figure 38.

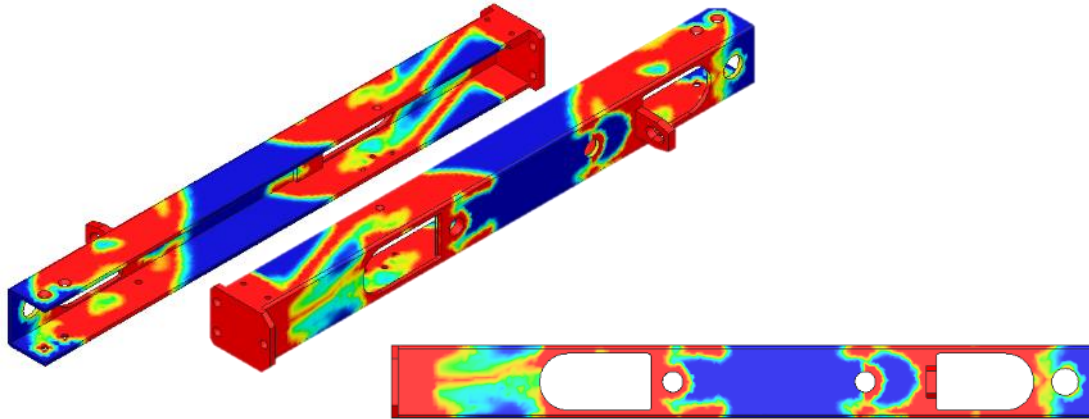


**Figure 38.** Geometry constrains.

Where:

1. Connections at the wagon.
2. General geometry constraints.
3. Adjustments bolts, holes needed for the assembly.

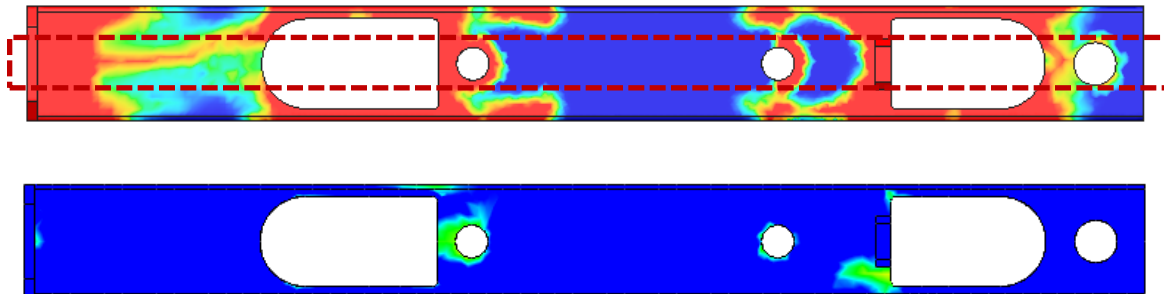
The results displayed in Figure 39 are consistent with the mesh characteristics used previously. The red areas correspond to the most critical path and the blue region, to the less loaded material, suggesting a lower thickness or a completely removal of the zone.



**Figure 39.** Load path identification at the ties

Some considerations are:

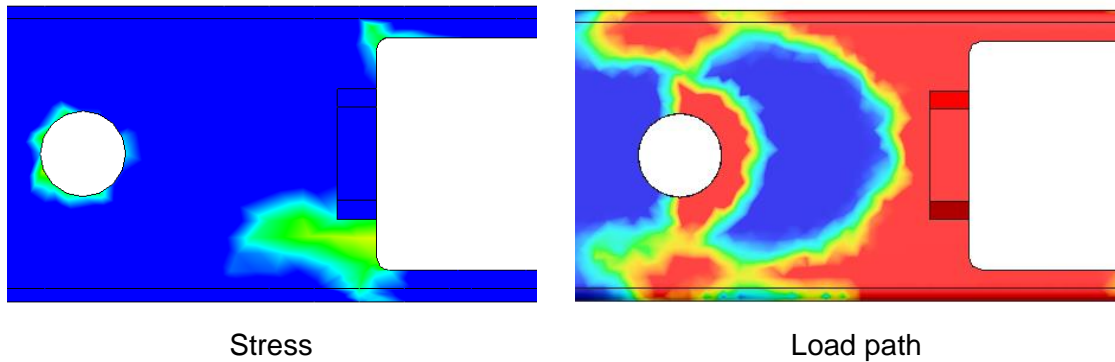
1. The most loaded material is located at the edges of the geometry and not in the middle of the “C” shape extrusion (red box located at Figure 40), with exceptions of the constrained regions.



**Figure 40.** Distribution along tie

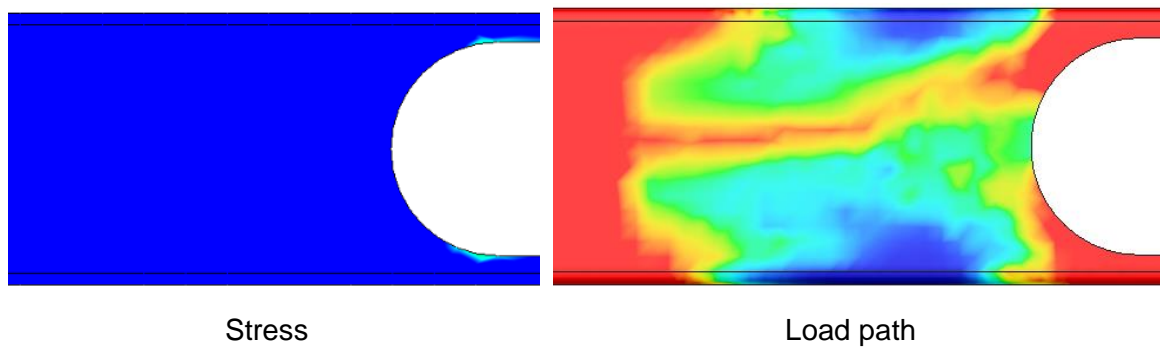
2. The region around the bracket is one of the most important and supports great stresses according to the FEA performed (Figure 41, left side), but juxtaposing the loading path, it is observable a blue region which does not coincides with any major loading and could be used in the manufacturing processes for any modification.





**Figure 41.** Comparison of the bracket

3. The zone observable in Figure 42 does not present high stresses as other areas but it is important because it links the different regions.
4. The critical areas identified in the computational simulation are linked with the loading path, as a verification method.



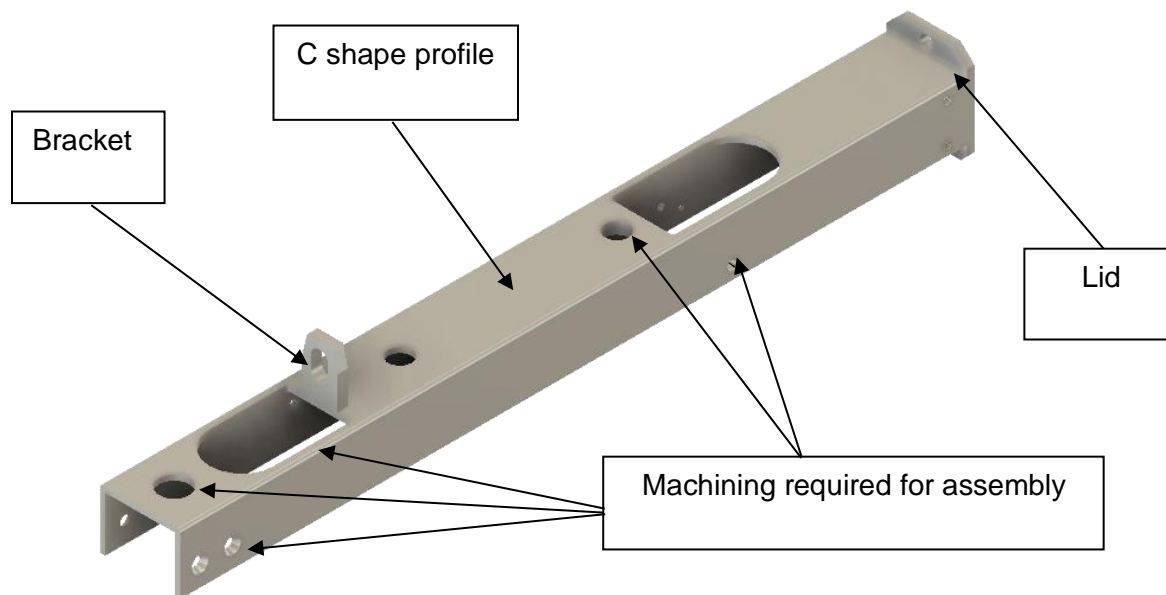
**Figure 42.** Comparison of a Tie section

The information above illustrates the operational requirements and construction characteristics needed to be fulfilled by the manufacturing and design process.

## 6.2 Fabrication of the Tie by FSW

### 6.2.1 Manufacturing considerations

Below are discussed the different manufacturing steps required to obtain a complete tie and features (Figure 43).



**Figure 43.** Features identified for the manufacturing process.

1. All materials used for the component, including tools and backing must be available locally or require a simple import process that does not involve minimum quantities or long waiting periods.
2. Tool's manufacture should be locally achievable to be replicable on site.
3. The low number of components required annually for this application (for an approximate total of 516) is a fundamental factor and one of the main criteria in selecting adequate manufacturing processes because it does not justify a considerable investment, such as specialized machinery, unconventional alloys, or custom-made extrusion dies.
4. Welding machine requirements for all stages must allow the use of existing milling and CNC machines, therefore only position control should be used during parameter

selection for FSW, and ideally no tilt angle, since this may restrict the available machinery for this application.

5. Parameter selection must also relate to local machine capabilities, therefore, no rotational or travel speed values above existing limits must be employed.
6. Backing bars and tooling elements must also remain as simple and cost-efficient as possible, again related to lower costs and the low number of parts required.

### 6.2.2 Material selection

With the chemical composition and hardness values of the original tie and complementing the information with the most common aluminum alloys used in the railway industry and their local availability. It was proposed a list of three different metals suited for the solicitation (Table 10), paired with their mechanical properties, commercialization geometry and type of availability.

**Table 10.** Aluminum comparison [62][63][66]

Material	Mechanical strength (MPa)		Geometry	Availability
	Tensile	Ultimate		
AA 6063 – T5	145	186	L shape – Bock – Plate	Imported, locally available
AA 7075 – T6	462	524		Imported
AA 6082 – T4	110	205		Imported

From the alternatives, the material selected was the AA 6082 – T4 because it gives an intermediate ultimate strength (higher than the values obtained by FEA analysis) and easiness to be acquired locally.

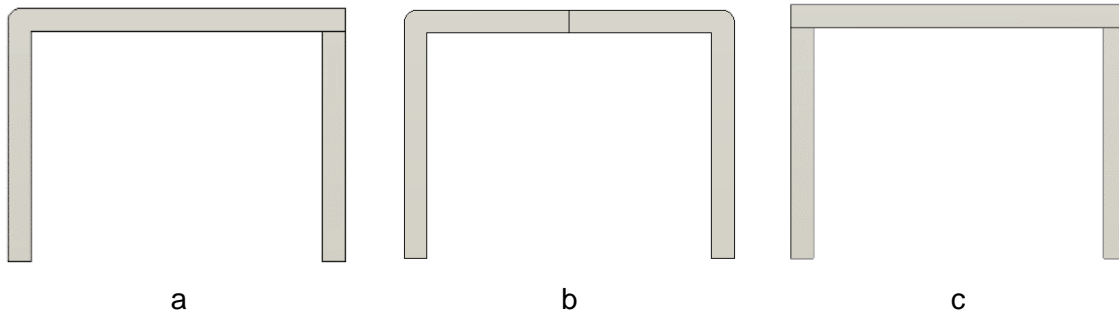
### 6.2.3 Design considerations

#### *U/C shaped profile*

Although an extruded profile presents multiple advantages, to obtain a tailormade shape involves a minimum volume which is prohibitive by the volumes and criteria exposed before. Additionally, a machined tie from a single block of aluminum is not well suited because the

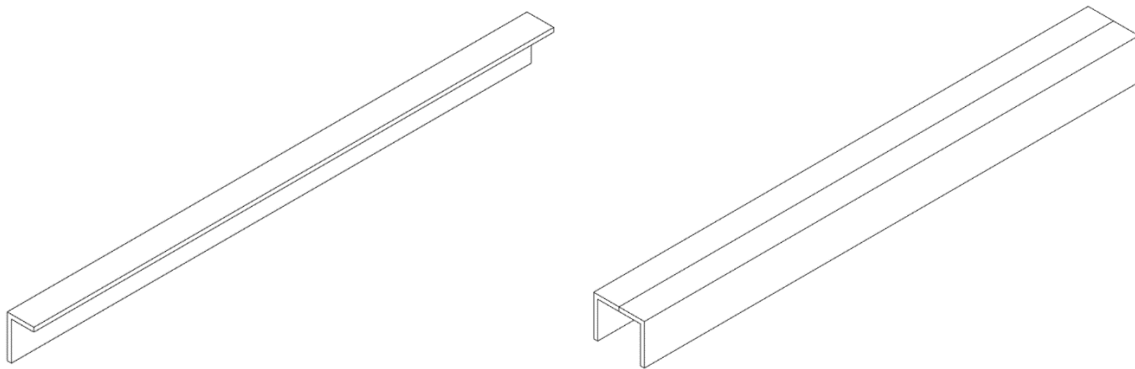
volume of waste metal is around 79%, extremely high compared to the fabrication using commercial extruded pieces.

So, it was decided to select from three configurations (Figure 44) the best possible distribution to implement FSW; aiming for less material waste, easier fixture and availability of components.



**Figure 44.** a) “L” profile and plate, b) two “L” profiles and c) three plates

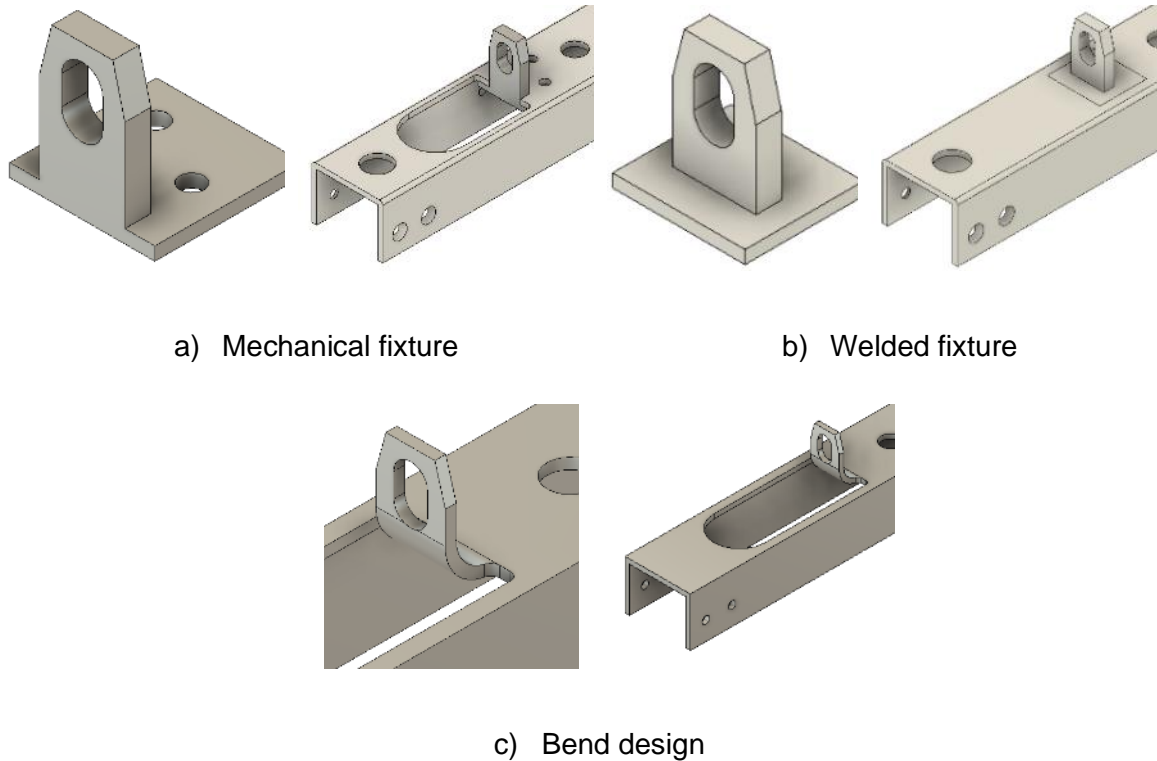
The selected design was the usage of two L shaped profiles in a butt joint configuration, as the sketches shown in Figure 45. This leads to the implementation of a traditional FSW tool, easier to manufacture locally and adequate to use in traditional machinery and finally in line with the considerations discussed before.



**Figure 45.** L- Shaped profiles

### **Bracket inserts**

For a selection of an adequate geometry that performs as discussed, three different options of brackets were evaluated (Figure 46) discarding the welded method used in the actual components and the usage of more complicated machinery like Linear Friction Welding (LFW). Those representations correspond to a mechanical, welded, and bent fixture.

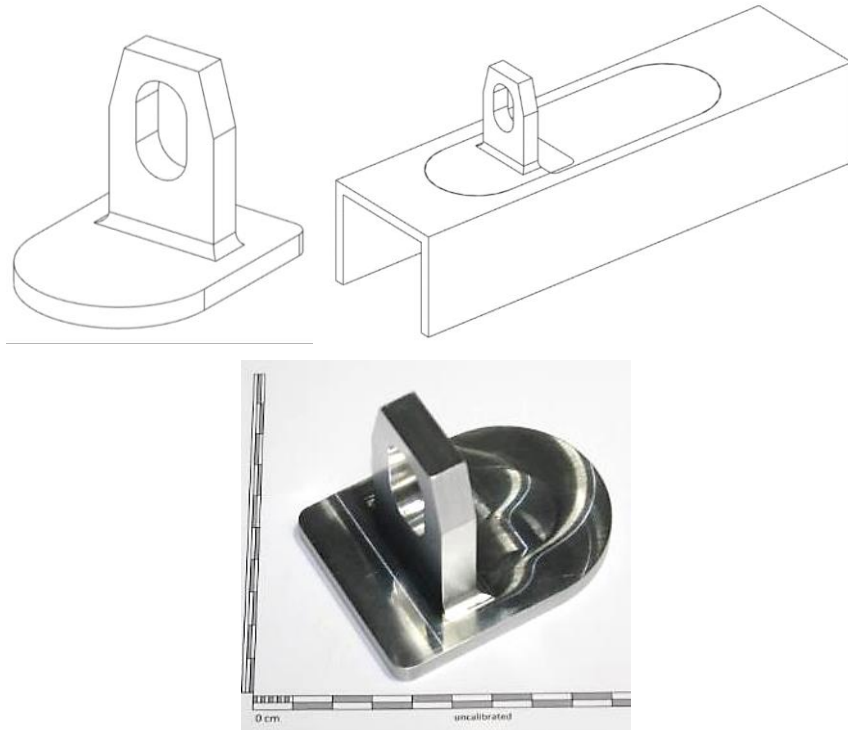


**Figure 46.** Types of brackets

For this part, the construction method chosen was by machining the Bracket, followed by welding around the base of it, taking a general idea the proposal exposed in Figure 46 - b.

This alternative was selected because it is easier to manufacture using FSW aiming to reduce the possible discontinuities observed in the original ties used in the door mechanism, moving the heat and mechanical affected zones farther from the stress concentrator geometry (the base of the bracket discussed in Figure 41). And it is easier to guarantee dimensional tolerances and lesser parts susceptible to defects, contrary to what happens with the bent and bolted design.

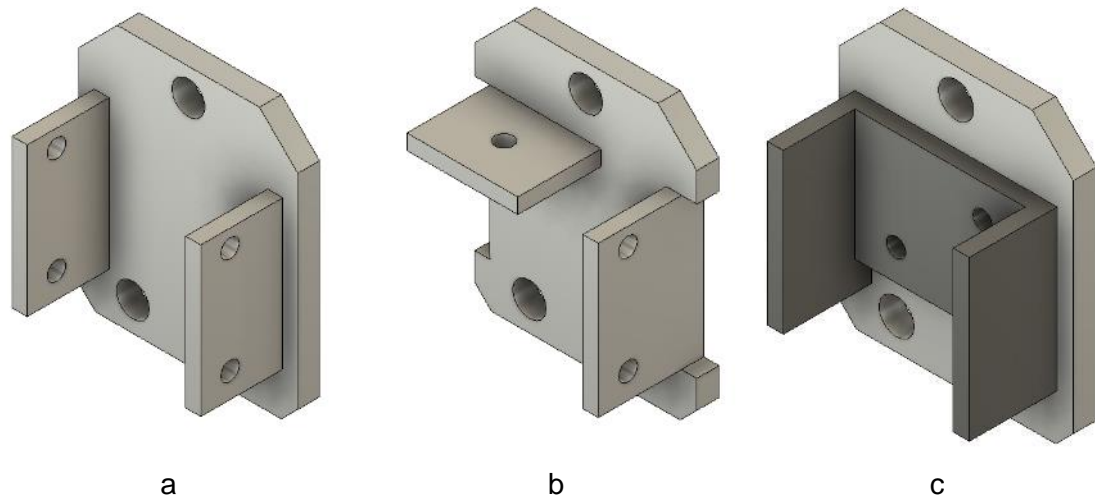
A schematic with the last iteration can be observed in Figure 47, where the base was modified to be rounded for an easier and without interruptions path of the tool. The location of the entrance and exit of the tool is set to following the required machining later.



**Figure 47.** From left to right: Insert, location and manufactured piece.

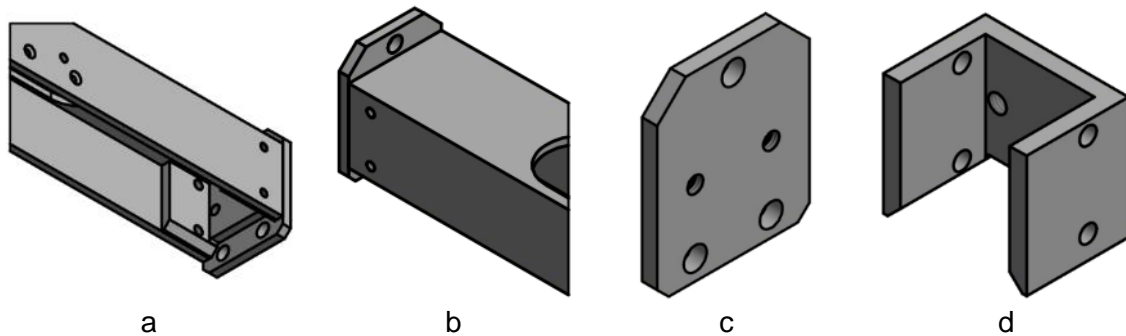
### *Lid*

For this geometry, an analogous method was implemented, proposing different manufacturing methods ranging from the implementation of FSW, using traditional arc welding methods or machining from a bulk of material. After the evaluation of the alternatives, available resources, and performance, three alternatives were proposed (Figure 48).



**Figure 48.** Lid models for assembly, a) Type 1 of mechanized lid, b) Type 2 of mechanized model and c) Modular type of lid.

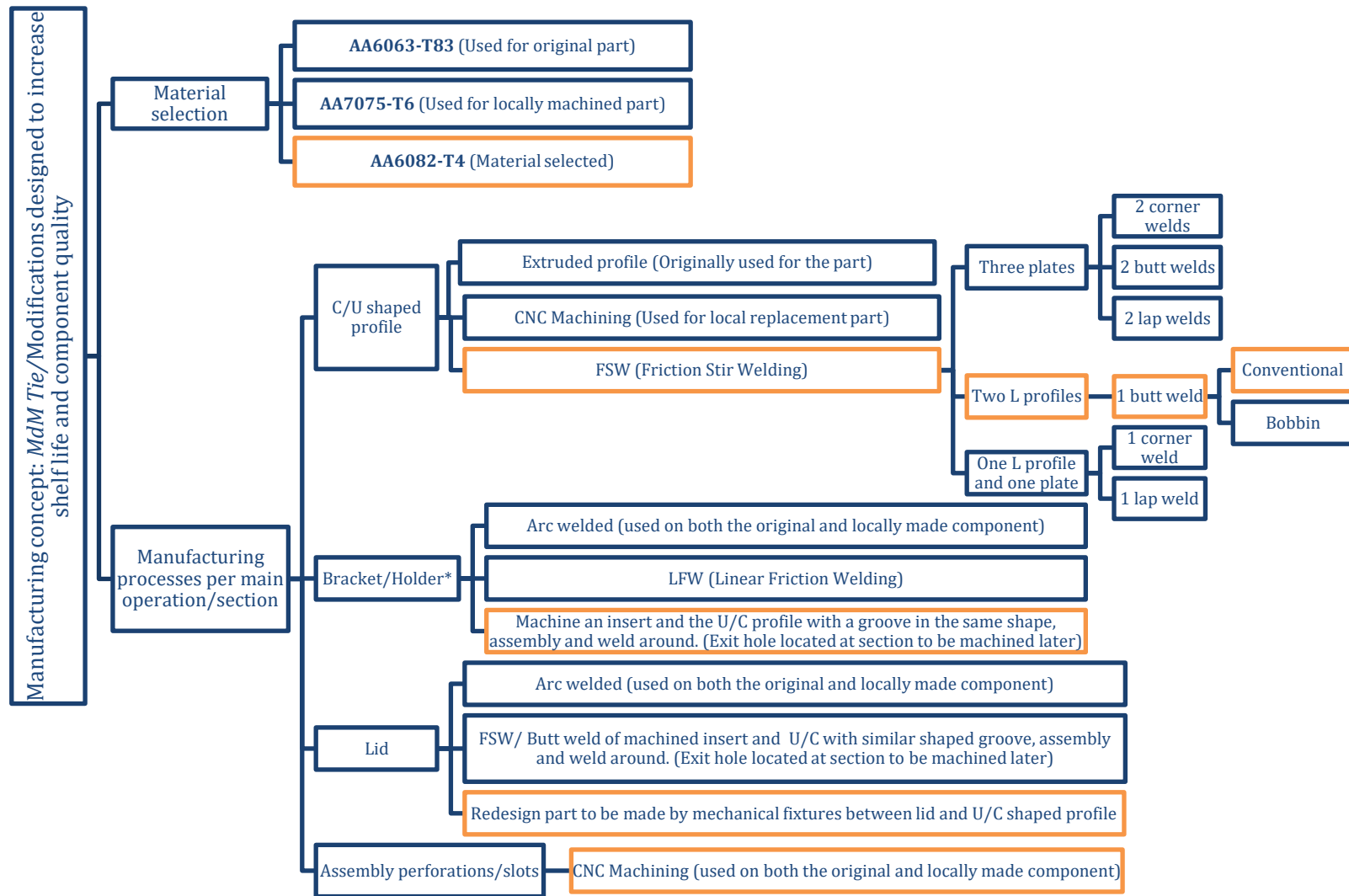
The selected design was the modular fixture (Figure 48 – c) because it can easily be replaced, uses the same perforations of the original tie and can be manufactured using other materials aiming for better tread support in a comparative manner against any aluminum alloy. In Figure 49 can be observed the final decisions made for its manufacture, having in consideration the bolted constrains and access for assembly.



**Figure 49.** Final Lid proposal. a) and b) represents the final component, c) Plate and d) “C” channel for mechanical assembly.

### *Assembly perforations / slots*

For the rest of the perforations in the component, CNC machining is the way to go to obtain the tolerances needed following the design of the original Ties. Figure 50 summarizes the design path described.



**Figure 50.** Summary of the manufacturing possibilities for the different stages in the construction of the tie.



## 6.2.4 Fixing and welding

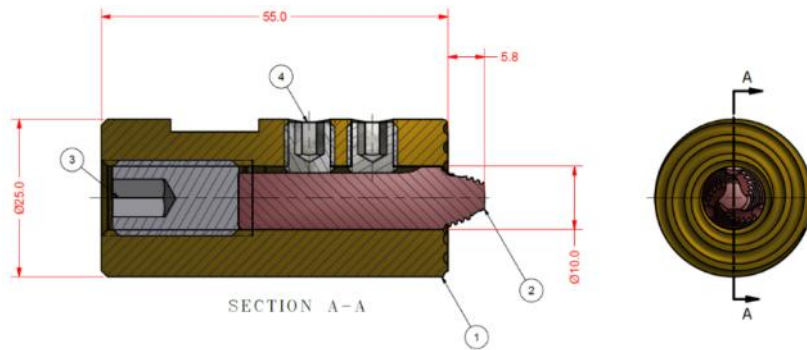
### *Setups, tools and parameters*

The selected and acquired L shape profile material, AA 6082 – T4, had dimensions of 2 ½" X 2 ½" by ¼" of thickness; which was machined to the adequate dimensions for the size of the tie and set up in a TTI FSW Machine to replicate a non-tilting fixture and position control displacement similar to an available CNC or milling equipment, comparable to the local manufacturing conditions (Figure 51). This machine was used because it is instrumented for force data acquisition required to evaluate the viability of the local implementation.



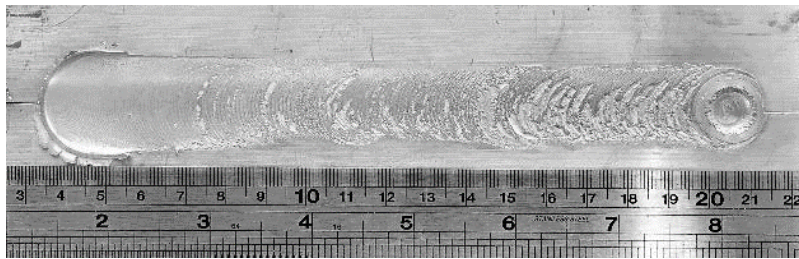
**Figure 51.** TTI disposition

Initial trials of the longitudinal weld were made using a Tri-flute tool as shown in Figure 52, with a threaded probe, 25 mm diameter shoulder with a scroll and 5,8 mm pin length. This design was previously built and tested by TWI for non-tilting welds (based on a tri-flute tool), and the parameters used were selected based on their prior experiences; 600 rpm and 600 mm/min.



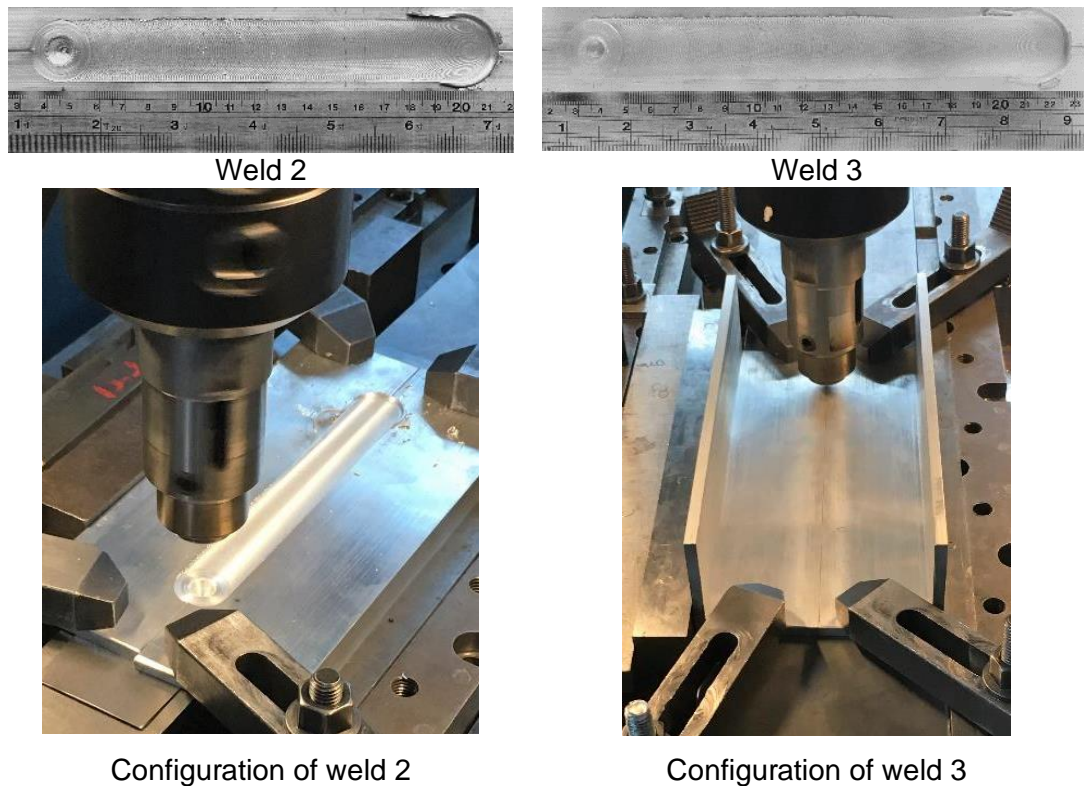
**Figure 52.** Initial tool for trials for longitudinal welds

A total of 5 welds in position control were made to verify the conditions and parameters selected, taking in place the requirements of the local available machinery. The first result obtained is observable in Figure 53, where the coarser finish is due to the initial set-up and was used as a guide for the following welds.



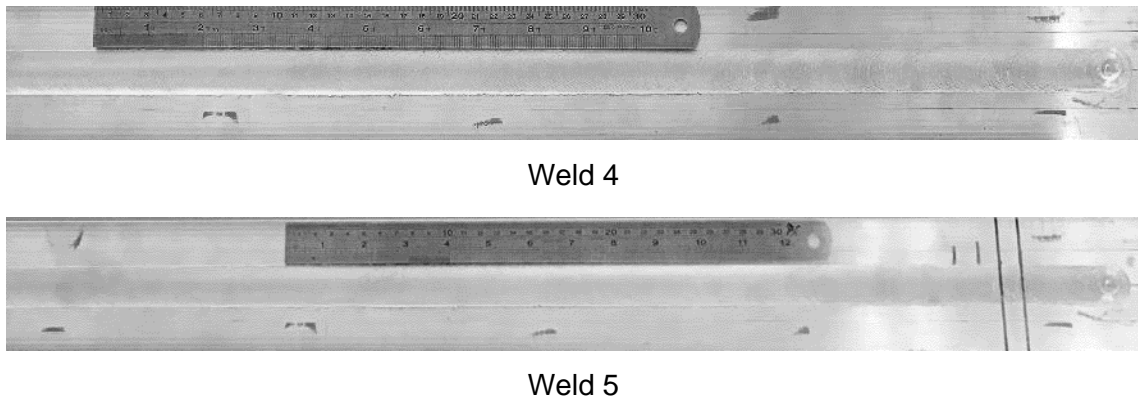
**Figure 53.** Weld 1

The next analysis was focused on the orientation of the L shape profiles, upwards or downwards relative to the backing plate as observable in Figure 54 for welds 2 and 3.



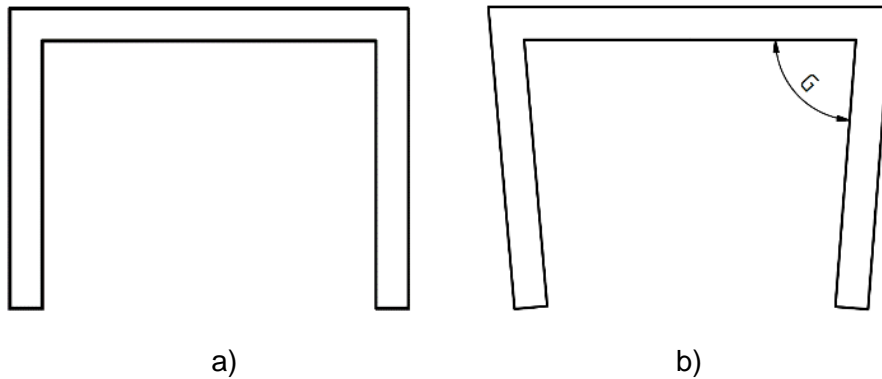
**Figure 54.** Results and configuration of welds 2 and 3

Thinking of later stages, the configuration corresponding to weld 2 was selected because facilitates assembly and helps the usage and access of the fixing components traditionally employed in machining applications. Welds 4 and 5 were made as replicas to obtain samples and used as a base material for subsequent trials for the following stages (Figure 55), having the final length required for the manufacture of the tie.



**Figure 55.** Final welds

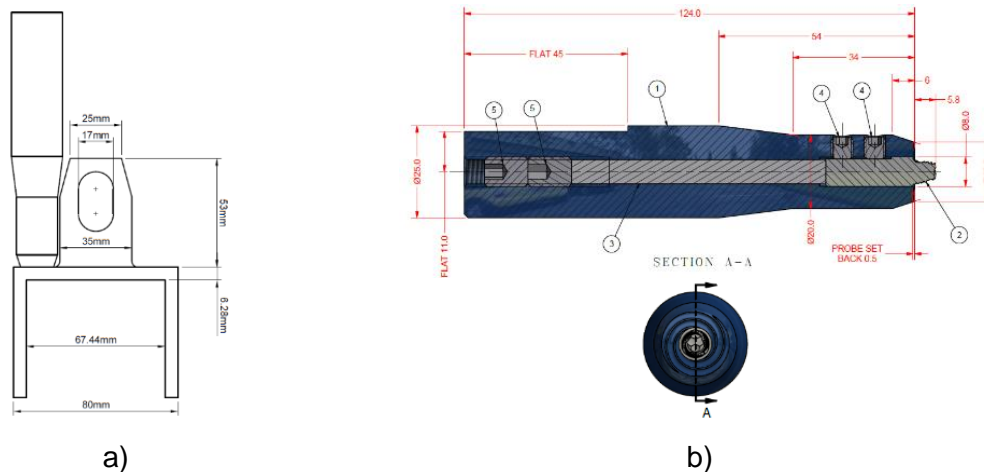
Some distortion was observed around the lateral faces in a slight manner without compromising the quality of the welds, like the exaggerated modification shown in the schematic of Figure 56. The dimensional alterations of the G angle are low enough, between 0.5 and 0.7 degrees, to be acceptable according to set tolerances required by MdM.



**Figure 56.** Post weld schematic distortion, a) expected result b) angular distortion obtained

### *Bracket insert*

For the welding proposed around the Bracket, a new tool with similar features to the initially described but with a smaller shoulder was required since the tolerances were tight to pass around the feature without compromising the tie (Figure 57). This new tool, if needed, can be also used for the longitudinal welds of the L-shaped aluminum profiles because it has the same material flow characteristics.



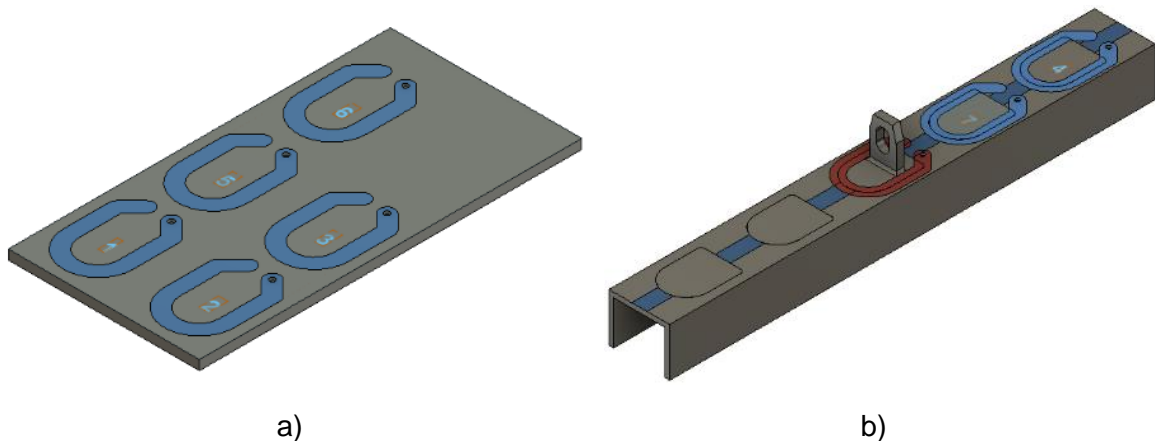
**Figure 57.** Tool - bracket disposition, a) tolerances needed and b) new tool.

Prior to performing any weld with the same parameters implemented for the longitudinal seam, it was needed to design a backing plate to guarantee the soundness of the seam during the execution of the FSW process. Two blocks as shown in Figure 58 were used, which are adjustable along the angled face until the dimensional accuracy is met.



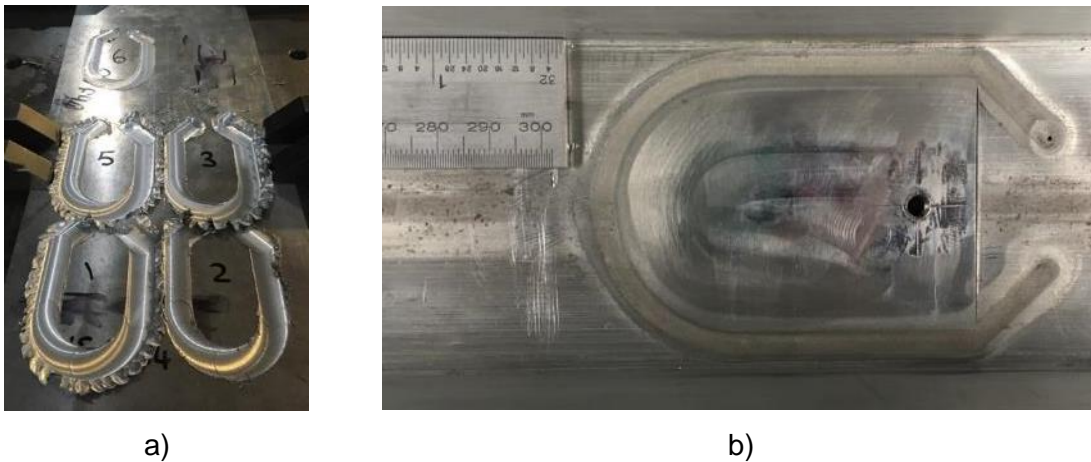
**Figure 58.** Backing design

To evaluate the weld pattern and the previous setup, it was proposed 7 preliminary welds on a plate and the “C” channel as presented in Figure 59, followed up by inserts without the bracket (red path) to evaluate the formation of flash and tool path, to finally obtain 2 of the expected results without any discontinuity.



**Figure 59.** Welds for the bracket, a) plate pattern and b) Tie welds

In the plate patterns, some of the parameters used left flash but the tie welds present a proper penetration and seam path as shown in Figure 60 - b.



a) b)  
**Figure 60.** Bracket welds, a) plate seams, b) back of the pattern

## 6.2.5 Forces during welding

### *Forces involved in the welds*

Having all the seams performed the Table 11 summarizes the most demanding welds due to their length for any machinery, the initial 5 longitudinal welds.

**Table 11.**Welding parameters Welds 1-5

Parameter/Information	Weld				
	1	2	3	4	5
X-Force (kN)	3,7	1,6	1,6	1,9	1,8
Y-Force (kN)	2,4	1,1	1,0	1,3	1,6
Z-Force (kN)	10,9	19,1	23,5	17,4	17,1
Spindle rotation speed (rpm)	601,6	601,3	601,4	601,5	601,3
Spindle traverse speed (mm/min)	599,9	600,0	600,0	600,0	600,0
Torque (Nm)	41,7	69,6	74,0	67,6	65,0
Weld length/Stable (mm)	122,5	121,4	141,1	709,3	777,5

### *Local providers*

A local evaluation of different providers was made (Table 12 [67]) to identify possible local industries that have the equipment to carry on the welding process according to the forces presented in Table 11.

**Table 12.** Local industries [67]

Local manufacturer	Contact number and website	Machines available	Capacities		
Industrias EDAFA S.A.S	+(57) (4) 279 52 46 www.edafasa.com	CNC machining center	Bed dimensions: 1016 x 508 mm Allowed workpiece height: 508 mm Max. workpiece weight: 680 kg		
		CNC milling machine	Bed dimensions: 500 x 300 mm Allowed workpiece height: 300 mm Max. workpiece weight: 250 kg		
		Maquinamos	+(57) (4) 448 49 98 www.maquinamos.com	CNC machining center	Bed dimensions: 1020 x 650 mm Allowed workpiece height: 620 mm Max. workpiece weight: 1 ton
				Gantry type milling machine	Bed dimensions: 1500 x 1000 mm Allowed workpiece height: 300 mm Max. workpiece weight: 2.5 ton
Industrias HRV	+(57) (4) 235 30 56 www.industriashrv.com	Conventional milling machine	Bed dimensions: 1500 x 500 mm Allowed workpiece height: 500 mm		

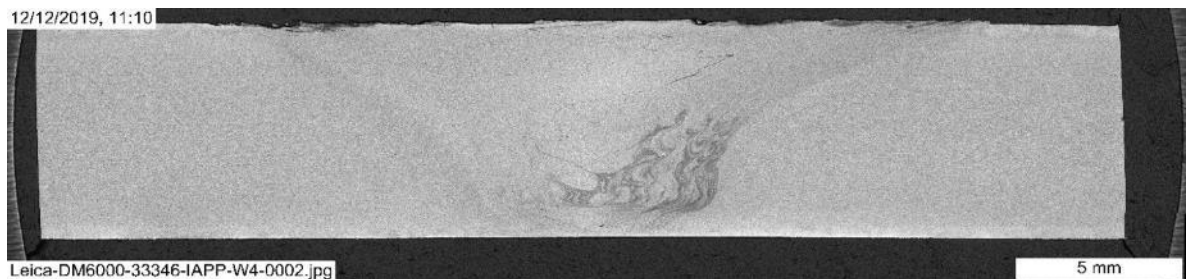
Local manufacturer	Contact number and website	Machines available	Capacities
Kreator Inc.	+(57) (4) 444 58 12 www.kreator.com.co	CNC milling machine	Max. workpiece weight: -
			Bed dimensions: 1016 x 406 mm
Industrias Famec	+(57) (4) 444 23 64 www.industriasfamec.com	CNC machining center	Allowed workpiece height: 406 mm
			Max. workpiece weight: 400 kg
Industrias Famec	+(57) (4) 444 23 64 www.industriasfamec.com	CNC machining center	Bed dimensions: 889 x 399 mm
			Allowed workpiece height: 508 mm
SAIT	+(57) (4) 288 40 28 www.sait.com.co	Universal vertical lathe	Max. workpiece diameter: 6300 mm
			Allowed workpiece height: 3200 mm
SAIT	+(57) (4) 288 40 28 www.sait.com.co	CNC machining center	Max. workpiece weight: 160 ton
			Bed dimensions: 8000 x 3000 mm
SAIT	+(57) (4) 288 40 28 www.sait.com.co	CNC machining center	Allowed workpiece height: 2500 mm
			Max. workpiece weight: 32 ton



## 6.3 Evaluation of welded samples

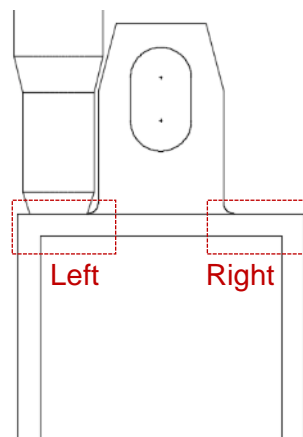
### 6.3.1 Samples and hardness evaluation

To evaluate the parameters and penetration of the tool used in the longitudinal seam, weld 4 (Figure 55) was sectioned and polished using *Emeril* paper from 600 to 300 grit and diamond polish, followed by a Keller reagent attack. The micrograph is presented in Figure 61, in which is observable a full tool penetration with no visible voids or another type of discontinuity as expressed in the ISO 25239-1:2011, like cavities and excessive thickness variation.



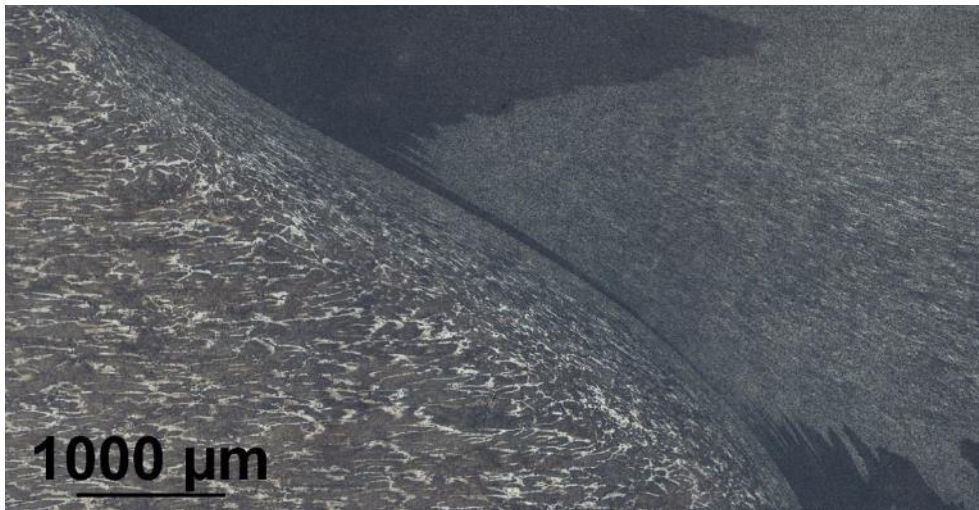
**Figure 61.** Weld 4 micrograph made by FSW, scale 5 mm.

The same analysis was made to the Bracket welds; two samples were cut from the left and right sides of the seam (Figure 62) and prepared in a similar manner to the longitudinal section.



**Figure 62.** Samples obtained from Bracket weld

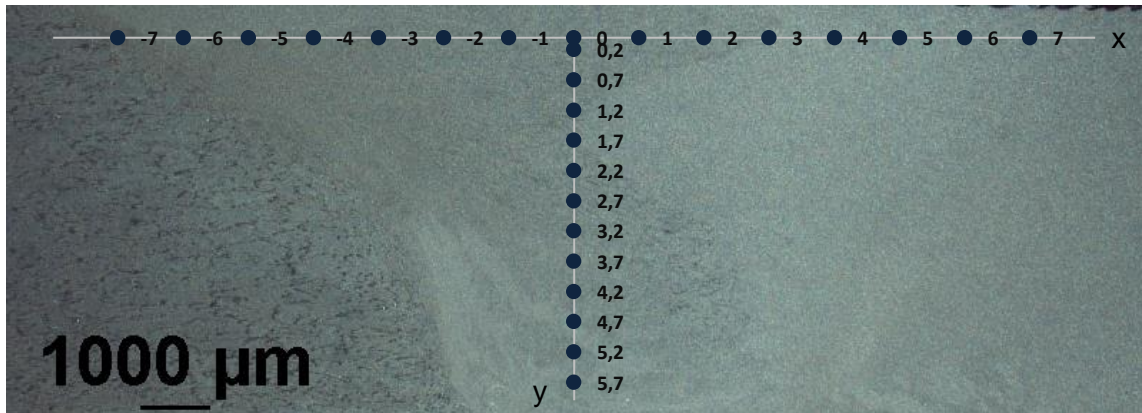
The results of the macrographs show no visible discontinuities as well as the longitudinal seam, corroborating that the parameters and tool are adequate for this material despite having a smaller shoulder. A closer evaluation of the microstructure (Figure 63) shows a material flow that goes from the top of the weld all the way to the bottom, consistent with the geometry and length of the tool's pin and clockwise rotation. The grains located at the edge of the stir zone presents the greatest mechanical deformation, a consequence of the dynamic recrystallization in comparison with the surrounding material. Additionally, it can be observed a "Z" or intercalated pattern consistent with the line of contact of the different metals through the thickness of the piece as reported by authors like M. Guerra et al and Ying Li, L.E. et al [68], [69].



**Figure 63.** Detailed microstructure of bracket weld by FSW, scale 1000 µm.

### 6.3.2 Hardness

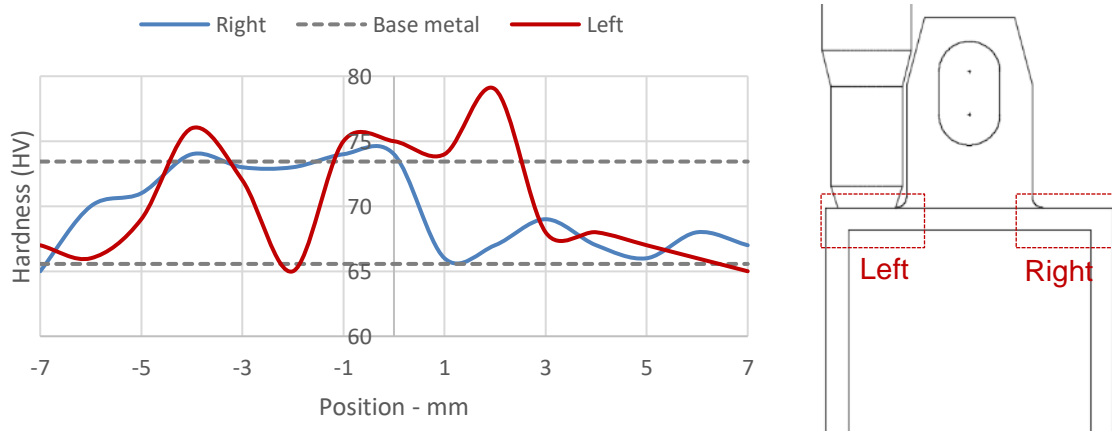
The micro-hardness data was obtained from the cross section of the Bracket samples following the pattern presented in Figure 64 and initially located from the top of the weld at 300 µm, aligned with the middle of the pin. Those values were obtained using an *Indenter* ZHµ machine, set to 300 grams and 10 s per sample.



**Figure 64.** Hardness indentations

The results obtained from the two welds follow the hardness pattern presented in Figure 65, where:

- The dotted lines correspond to the base metal values of the AA 6082 – T4 used for welds, between 65,6 HV and 73,4 HV with a standard deviation of 3,9 HV and an average of 69,5 HV; in correspondence of the 65 HV reported for the material [70].
- The red line corresponds to the values obtained along the x-axis on the right (Figure 65).
- The blue line corresponds to the values obtained along the x-axis on the left side (Figure 65).



**Figure 65.** Vickers hardness pattern on the x axis and welds samples evaluated

The results show a similar behavior comparing the advance and retreating sides, where the hardness tends to be greater on the first one, exceeding in some cases the average value. It is necessary to understand that in the right weld, the east side from the middle of the pin is called the advance region because the tool rotates counterclockwise, and on the left side is the opposite. All the values are around the average band of hardness.

Applying the relationship between hardness and strain proposed by Cahoon et al. for aluminum alloys [71], expressed in equations 10 and 11 as a way to relate the values obtained with an efficiency of the joint; the results are on average  $S_{0,002} = 132.16 \text{ MPa}$  and  $S_u = 215.25 \text{ MPa}$ . Which corresponds to a proficiency above 95% respect the base material [70][72].

$$10) S_u = 9.81 * \frac{VHN}{2,9} \left( \frac{n}{0,217} \right)^n$$

$$11) S_{0,002} = 9.81 \frac{VHN}{3} (0,1)^n$$

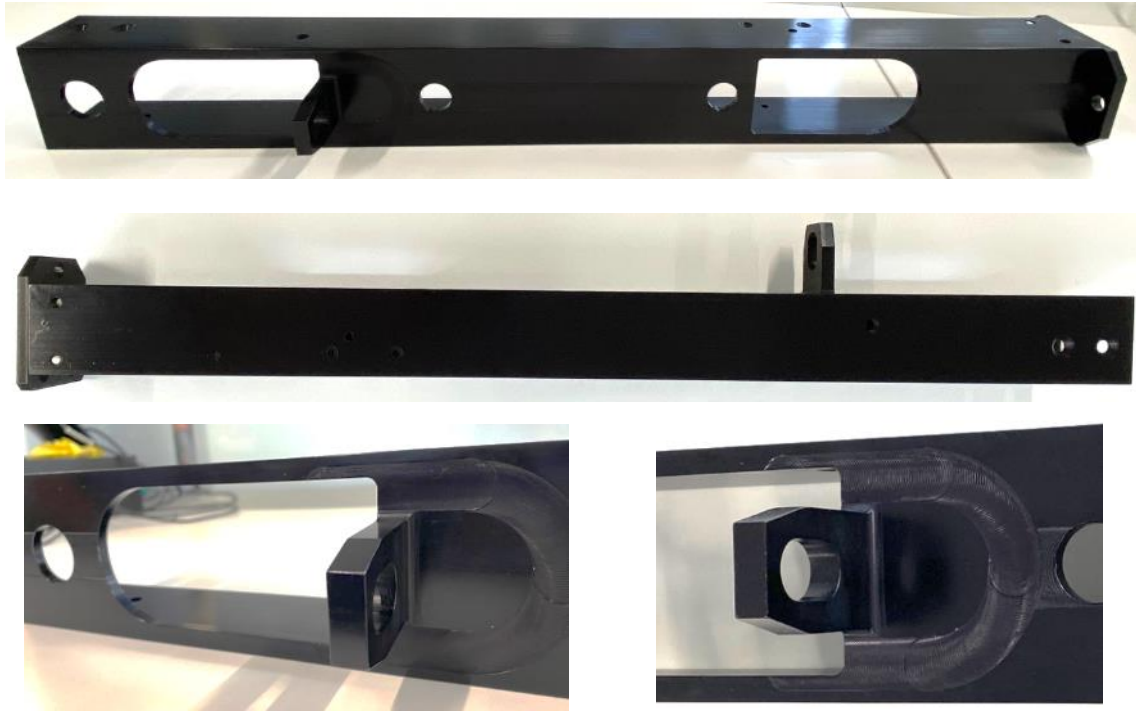
Where

- $VHN$  is the harness in Vickers.
- $n$  is the strain-hardening coefficient, for aluminum is 0,203 [73].
- $S_u$  is the ultimate strength.
- $S_{0,002}$  is the yield strength.

This information helps to conclude that the used tool and parameters are adequate to obtain welds with great mechanical response, not much different from the base material used.

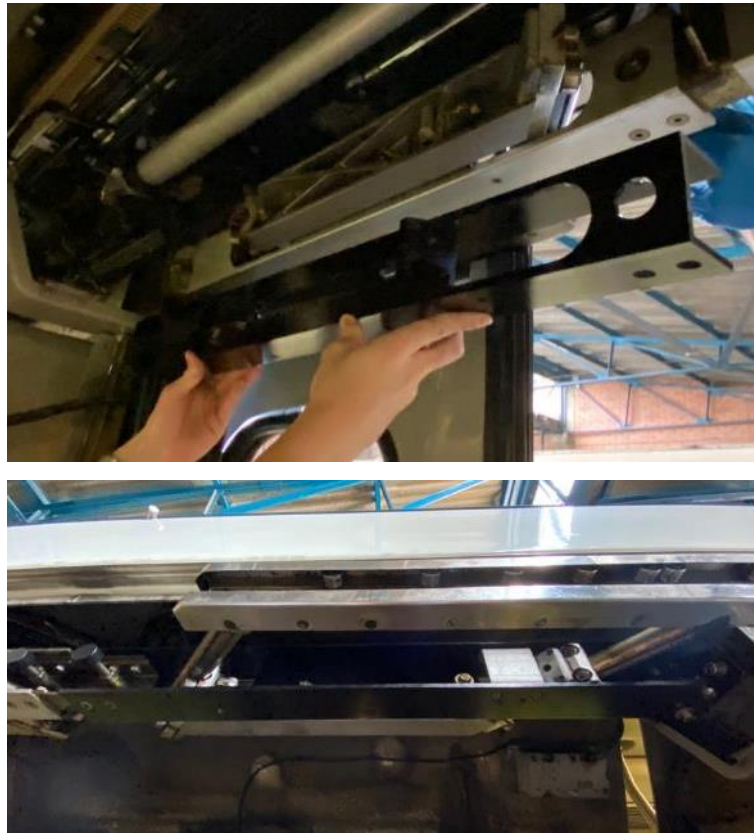
### 6.3.3 Prototype component

A first prototype was manufactured implementing the considerations exposed before. The component is observable in Figure 66 and was anodized only for a better presentation.



**Figure 66.** Tie prototype

As mentioned before, the FSW does not need any post-processing to have a great superficial finish and keep the dimensional accuracy. Having that in mind, the component was placed at the door as shown in Figure 67 to evaluate its performance and the surface finish used as reference for further visual inspections.

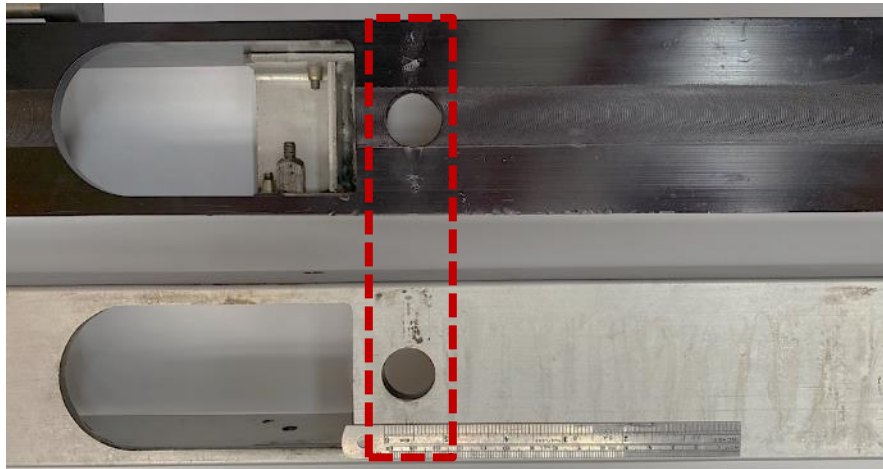


**Figure 67.** Tie installation at wagon.

### **6.3.4 Prototype inspection**

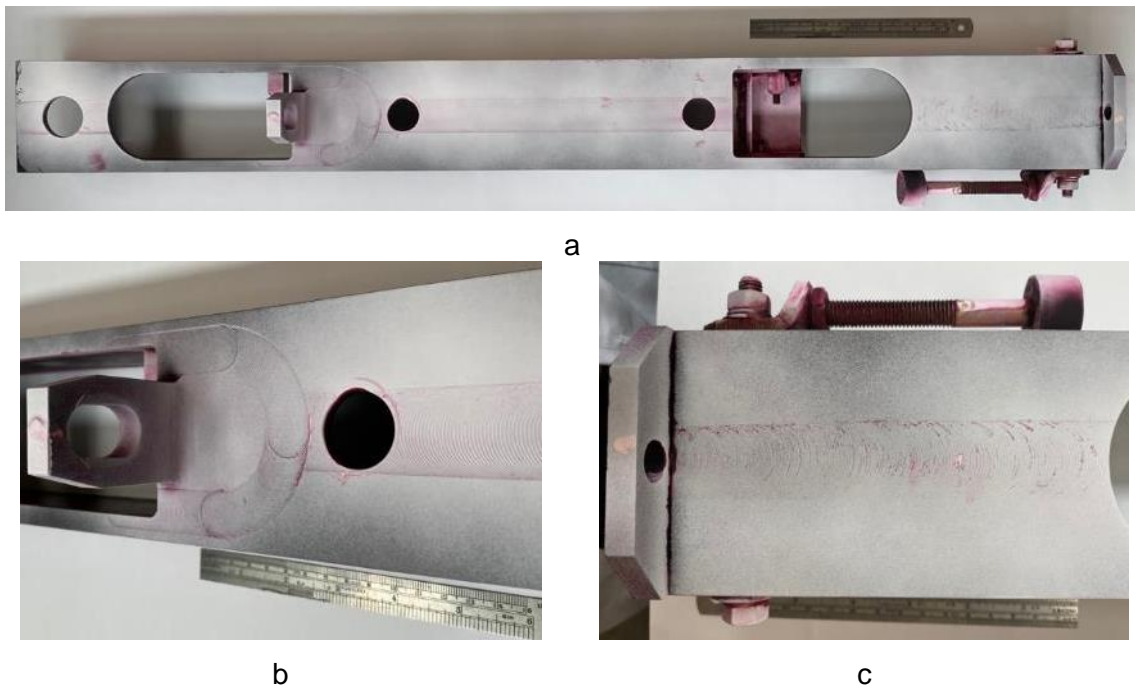
Because the prototype was installed in a door assembly, after approximately 5 months of operation representing 1540 cycles, the tie was disassembled and cleaned for an initial visual inspection (VI), followed by a dye penetrant (DP) analysis using Spotecheck® consumables aiming to evaluate the performance of the welds in a preliminary way, followed by a reassembly which has not presented any concern at the present time.

During the VI it was observable scratches and deformations around the bolted connections as expected, but a major deformation was identified near one of the holes. A comparison was made between the prototype and an older component, which reflected the same discontinuity with a minor severity (Figure 68) but does not represent any problem at the time.



**Figure 68.** Deformation

The dye penetrant analysis was performed all over the outside and inside of the component and the general results obtained are shown in Figure 69. Where most of the dye is located around the crest of the weld but not on a visible crack or discontinuity was observed which could jeopardize the component.



**Figure 69.** DP examination, a) general inspection, b) closeup of the Bracket and c) closeup of the Lid

---

## 6.4 Welding procedure

After evaluating all the considerations for the manufacture of the Tie, a welding procedure specification (WPS) was constructed following the AWS D17.3 template and guidelines [41] for the “C” channel (Table 13) and Bracket (Table 14). A small summary is presented below, detailing the specific information regarding the welding procedure.

- **Background**

The information presented in this section identifies the governing code selected based on the information presented before. For this application, the chosen code is AWS 17.3 because is stricter compared with the ISO, selecting class A because any underperformance of this component will put in danger the people using the mass transportation system.

- **Sketch of joint Design**

The information regarding the weld is presented in the sketches presented in both tables, those figures present the welding region in a different color.

- **Set-up**

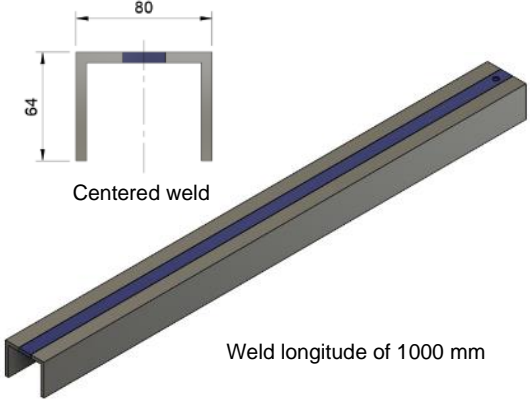
Both welds are proposed in a butt weld configuration as presented, for this welding application, it is necessary no gap (requiring the previous machining) to guarantee the lack of inner discontinuities in the seam.

- **Welding variables**

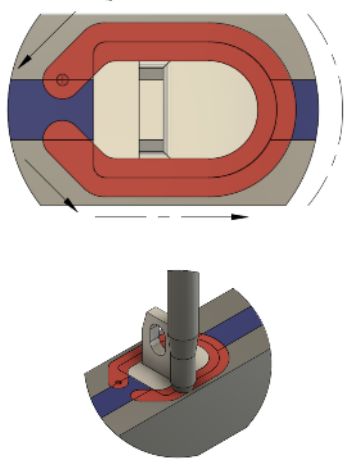
Finally, the information presented supports the arguments of no tilting of the tool due to local requirements, traveling and rotational speeds and maximum force during welding, required for selecting machinery strong enough to withstand the processes forces.



**Table 13.** Welding Procedure Qualification Record for Friction Stir Welding – longitudinal weld.

	Date: 19-02-2021	
Governing Code: AWS D17.3	WPS No.: 001	
Friction Stir Welding Method: Conventional	Engineer: Santiago Escobar Muñoz	
<b>Background</b>	<b>Sketch of Joint Design</b>	
Part: Structural component door mechanism		
Weld Class: A		
<b>Aluminum Alloys</b>		
Alloy 1: AA 6082 Temper: T4 Thickness Range (in [mm]): 1/4" [6,35 mm]		
Alloy 1: AA 6082 Temper: T4 Thickness Range (in [mm]): 1/4" [6,35 mm]		
Grain Direction: In line with weld		
Preweld Cleaning: Yes with degreaser or wire brush if needed		
Root Face or Surface Coating: No		
<b>Set-up</b>		<b>Welding variables</b>
Weld Tool Drawing Number: N/A		Axial Force (lbs [kN]): 2473 [11,4]
Weld Joint Type: Butt joint	Spindle Speed (R/MIN): 600	
Joint Gap (in [mm]): 0 [0]	Direction of Tool Rotation: Clockwise	
Tool Offset (in [mm]): 0 [0]	Tilt Angle (degrees): 0°	
Weld Fixture Drawing Number: N/A	Plunge Speed (in [mm] / min): 1,18 [30]	
Anvil Material: ASTM A29 Grade 4340	Dwell Time (s): 20	
	Clamp Pressure (psi [kPa]) : N/A	
	Travel Speed (in [mm]/min): 23,6 [600]	
<b>Additional Considerations</b>		
It is required to evaluate the transitions zones of the weld; the 1000 mm length takes into consideration the discard zones.		

**Table 14.** Welding Procedure Qualification Record for Friction Stir Welding – Bracket weld

	Date: 19-02-2021
Governing Code: AWS D17.3	WPS No.: 002
Friction Stir Welding Method: Conventional	Engineer: Santiago Escobar Muñoz
<b>Background</b>	<b>Sketch of Joint Design</b>
Part: Structural component door mechanism	<p style="text-align: center;">Weld around red path</p> 
Weld Class: A	
<b>Aluminum Alloys</b>	
Alloy 1: AA 6082 Temper: T4 Thickness Range (in [mm]): 1/4" [6,35 mm]	
Alloy 1: AA 6082 Temper: T4 Thickness Range (in [mm]): 1/4" [6,35 mm]	
Grain Direction: N/A	
Preweld Cleaning: Yes	
Root Face or Surface Coating: No	
<b>Set-up</b>	<b>Welding variables</b>
Weld Tool Drawing Number: N/A	Axial Force (lbs [kN]): 2473 [11,4]
Weld Joint Type: Butt joint	Spindle Speed (R/MIN): 600
Joint Gap (in [mm]): 0 [0]	Direction of Tool Rotation: Clockwise
Tool Offset (in [mm]): 0 [0]	Tilt Angle (degrees): 0°
Weld Fixture Drawing Number: N/A	Plunge Speed (in [mm] / min): 1,18 [30]
Anvil Material: ASTM A29 Grade 4340	Dwell Time (s): 20
	Clamp Pressure (psi [kPa]): N/A
	Travel Speed (in [mm]/min): 23,6 [600]
<b>Additional Considerations</b>	
It is necessary to evaluate acceleration ramps for every direction change. Additionally, the start and finish of the welds are located in the zone which will be removed later in the fabrication; thus, those transition zones are discarded.	

For further information regarding the steps required for the welding of the Tie, refer to Annex 4 – Welding steps.

---

## 7. Conclusions

In this project, the structural member of the door opening mechanism selected from the MAN trains called *tie* was evaluated using analytical and computational tools to assess its manufacture, mechanical requirements, and failure zones. Those results are aligned with the notorious discontinuities identified by visual inspection.

The main reason identified for the failure of the component is the high stresses around the heat affected zones left by the welds and section changes along the channel, reflected in cracks longer than 10 mm, which coincide with the more critical zones obtained by the computational analysis (around the Bracket and Lid); exacerbated by the fatigue of the material during cyclic normal operation (more than 92 thousand rounds per year).

The areas of higher stress obtained using the FEA analysis were compared in conjunction with the topological optimization performed, making it possible to identify the material with lower mechanical loading and used for the intended redesign. This finally helped to construct a different approach to manufacture the component using Friction Stir Welding (FSW) as an alternative for joining two commercially available “L” shaped aluminum extrusions and other machined parts (made from the AA6082-T4 alloy) in a butt joint configuration, to withstand the mechanical loading required.

To understand the regional limitations, the evaluation of forces and other parameters to understand the regional limitations helped to identify local possible manufacturers which could use their existing machinery without any significant investment.

Successful preliminary welds were manufactured using the parameters, 600 RPM and 600 mm/min, presenting no discontinuities and cavities with an average hardness of 69.5 HV in line with the tolerances of the base material 65 HV value [70]. Leading to construct a welding procedure with the design considerations to guarantee sound welds.

A prototype was manufactured and tested on the actual door mechanism without presenting any discontinuities after 5 months of operation and more than 1540 cycles, corroborating the feasibility of the welding process and design considerations for this kind of applications using aluminum alloys and local equipment.

Having all the information in consideration and the adequate results obtained, it was possible to propose a manufacturing and welding procedure for this specific component, which not only could help its local construction but also opens new possibilities to produce other pieces using this work as a guide.

New lines of research and development around other transportation systems could be interesting to be evaluated in future works, like ground and fluvial means, due to the similarities their components manufacture, materials usage and availability local knowledge in comparison with the railway industry.

---

## 8. References

- [1] Semana, “Ferrocarriles, ¿al borde de la muerte?,” *Tendencias*, 2018.
- [2] A. de Bogotá, “Proyecto Primera Línea del Metro de Bogotá,” *Metro de Bogotá*, 2019.
- [3] El Colombiano, “Lo que sigue para el metro de la 80 tras firma de convenio con la Nación,” *Antioquia*, Medellín, p. 1, Nov. 30, 2020.
- [4] G. Vargas Lleras *et al.*, “PMTI,” 2015. [Online]. Available: [https://www.ani.gov.co/sites/default/files/u233/pmti\\_entregable\\_1\\_final\\_nov11.pdf](https://www.ani.gov.co/sites/default/files/u233/pmti_entregable_1_final_nov11.pdf).
- [5] E. Colombiano, “¿Qué hará el Metro con los trenes más antiguos?,” *Antioquia*, p. 1, 2018.
- [6] Metro de Bogotá, “Cada vez más cerca el inicio de las obras del metro de Bogotá: firmado el contrato de interventoría,” Aug. 2020. <https://www.metrodebogota.gov.co/?q=noticias/firmado-contrato-interventoria> (accessed Aug. 30, 2020).
- [7] El Tiempo, “La ruta para que Medellín tenga su tercera línea de Metro - Medellín - Colombia - ELTIEMPO.COM,” *Medellín*, p. 1, Apr. 02, 2020.
- [8] Metro de Medellín, “Listo aval fiscal para el Metro de la 80,” *Noticias Metro*, Mar. 17, 2018. <https://www.metrodemedellin.gov.co/al-día/noticias-metro/artmid/6905/articleid/1183/listo-aval-fiscal-para-el-metro-de-la-80> (accessed Aug. 30, 2020).
- [9] Metro de Medellín, “Proyectos METRO que se materializan en el campo de la innovación,” *Periódico Nuestro METRO*, 2018. .
- [10] O. T. Ola and F. E. Doern, “Fusion weldability studies in aerospace AA7075-T651 using high-power continuous wave laser beam techniques,” *Mater. Des.*, vol. 77, pp. 50–58, 2015, doi: 10.1016/j.matdes.2015.03.064.
- [11] D. Arizmendi, “Metro de Medellín invierte en investigaciones universitarias,” *Caracol Radio*, p. 1, 2011.
- [12] Metro de Medellín, “Innovación y creatividad de la mano del buen servicio,” Medellín, 2015.
- [13] J. Davenport and S. W. Kallee, “FRICTION STIR WELDING - A COMPETITIVE NEW JOINING OPTION FOR ALUMINIUM ROLLING STOCK MANUFACTURERS,” *European Railway Review Magazine*, Oct. 2002.
- [14] F. Franco, H. Sánchez, D. Betancourt, and Orlanis Murillo, “Soldadura por fricción-

- agitacion de aleaciones ligeras – una alternativa a nuestro alcance,” *Supl. la Rev. Latinoam. Metal. y Mater.*, vol. 1, no. 3, pp. 1369–1375, 2009, [Online]. Available: <http://www.rlmm.org/archivos/S01/N3/RLMMArt-09S01N3-p1369.pdf>.
- [15] E. Hoyos, D. López, and H. Alvarez, “A phenomenologically based material flow model for friction stir welding,” *Mater. Des.*, vol. 111, pp. 321–330, 2016, doi: 10.1016/j.matdes.2016.09.009.
- [16] S. P. Pérez, I. M. Insignares, C. O. Charris, J. Posada, and J. U. Silgado, “Medición Del Torque Durante La Soldadura Por Fricción–Agitación De Aluminio Mediante Un Sistema De Detección Con Transmisión En Tiempo Real,” *Rev. Colomb. Mater.*, no. 5, pp. 244–249, 2014, [Online]. Available: <http://aprendeonline.udea.edu.co/revistas/index.php/materiales/article/view/19226>.
- [17] J. Zapata, M. Toro, and D. López, “Residual stresses in friction stir dissimilar welding of aluminum alloys,” *J. Mater. Process. Technol.*, vol. 229, pp. 121–127, 2016, doi: 10.1016/j.jmatprotec.2015.08.026.
- [18] M. de Medellín, “El Metro ya cuenta con 21 trenes más,” *Noticias Metro*, 2018. .
- [19] Global Mass Transit Report, “Metro de Medellín to refurbish 42 MAN trains,” *Latin America News*, Jun. 09, 2018. <https://www.globalmasstransit.net/archive.php?id=30485> (accessed Aug. 31, 2020).
- [20] TWI, “What is the Heat Affected Zone (HAZ)?,” *Technical Knowledge*, 2021. <https://www.twi-global.com/technical-knowledge/faqs/what-is-the-heat-affected-zone> (accessed May 14, 2021).
- [21] TWI, “Friction Stir welding,” *Technical Knowledge*, 2019. .
- [22] R. S. Mishra and Z. Y. Ma, “Friction stir welding and processing,” *Mater. Sci. Eng. R Reports*, vol. 50, no. 1–2, pp. 1–78, 2005, doi: 10.1016/j.mser.2005.07.001.
- [23] P. Cavaliere, “Friction stir welding of Al alloys: Analysis of processing parameters affecting mechanical behavior,” *Procedia CIRP*, vol. 11, pp. 139–144, 2013, doi: 10.1016/j.procir.2013.07.039.
- [24] ISO, “25239-1:2011: Friction stir welding — Aluminium Part 1 : Vocabulary.” 2011.
- [25] AWS. American Welding Society, “Specification for Friction Stir Welding of Aluminum Alloys for Aerospace Applications,” 2010.
- [26] P. Kah, R. Rajan, J. Martikainen, and R. Suoranta, “Investigation of weld defects in friction-stir welding and fusion welding of aluminium alloys,” *Int. J. Mech. Mater. Eng.*,

- vol. 10, no. 1, 2015, doi: 10.1186/s40712-015-0053-8.
- [27] S. Kou, *Welding Metallurgy, 2nd Edition*. 2003.
- [28] Sapa Group, “Friction Stir Welding,” *Frict. Stir Weld. Advert. Doc.*, 2012, doi: 10.1533/9781845697716.
- [29] TWI, “Aluminium alloys,” *Aluminum alloys*, 2019. <https://www.twi-global.com/technical-knowledge/job-knowledge/weldability-of-materials-aluminium-alloys-021> (accessed Feb. 12, 2021).
- [30] TWI, “Job Knowledge 21,” *Aluminum alloys*, 2019. .
- [31] TWI, “I keep getting porosity when welding aluminium. Any advice?,” 2021. <https://www.twi-global.com/technical-knowledge/faqs/faq-i-keep-getting-porosity-when-welding-aluminium-any-advice>.
- [32] Q. LI *et al.*, “Segregation in fusion weld of 2219 aluminum alloy and its influence on mechanical properties of weld,” *Trans. Nonferrous Met. Soc. China (English Ed.)*, vol. 27, no. 2, pp. 258–271, 2017, doi: 10.1016/S1003-6326(17)60030-X.
- [33] K. Huang and R. E. Logé, “A review of dynamic recrystallization phenomena in metallic materials,” *Materials and Design*, vol. 111. Elsevier, pp. 548–574, Dec. 05, 2016, doi: 10.1016/j.matdes.2016.09.012.
- [34] S. Escobar and J. E. Guzman, “DESARROLLO DE MAPA DE PROCESOS PARA FRICTION STIR WELDING (FSW) DE LA ALEACIÓN COMERCIAL DE ALUMINIO AA7075 – T6.,” University EIA, 2017.
- [35] S. Lomolino, R. Tovo, and J. Santos, “On the fatigue behaviour and design curves of friction stir butt-welded Al alloys,” vol. 27, pp. 305–316, 2005, doi: 10.1016/j.ijfatigue.2004.06.013.
- [36] TWI, “Friction Stir Welding,” *Job Knowledge*, 2019. <https://www.twi-global.com/technical-knowledge/job-knowledge/friction-stir-welding-147>.
- [37] ISO, “25239-4:2011: Friction stir welding — Aluminium Part 4 : Specification and qualification of welding procedures.” 2011.
- [38] ISO, “25239-2:2011: Friction stir welding — Aluminium Part 2 : Design of weld joints.” 2011, [Online]. Available: <https://bsol-bsigroup-com.libezproxy.open.ac.uk/Bibliographic/BibliographicInfoData/0000000003017112>.
- [39] ISO, “25239-3:2011: Friction stir welding — Aluminium Part 3: Qualification of welding operators.” 2011.

- 
- [40] ISO, "25239-5:2011: Friction stir welding — Aluminium Part 5 : Quality and inspection requirements." 2011.
- [41] American Welding Society, *AWS D17.3/D17.3M:2016 - Specification for Friction Stir Welding of Aluminum Alloys for Aerospace Applications*. 2016.
- [42] W. M. Thomas, E. D. Nicholas, J. C. Needham, M. G. Murch, and P. Temple-smith, "Improvements relating to friction welding," WO1993010935 A1, 1993.
- [43] M. Kumagai and S. Tanaka, "Properties of aluminum wide panels by friction stir welding," *1st Int. Symp. FSW*, 1999.
- [44] H. Ohba, C. Ueda, and K. Agatsuma, "Innovative vehicle - The 'A-train,'" *Hitachi Rev.*, vol. 50, no. 4, pp. 130–133, 2001.
- [45] O. Blach and F. Senne, "Reibrührschweißen aus der Sicht eines Anwenders im Schienenfahrzeugbau," *2nd GKSS Work.*, 2002.
- [46] X. Liu, H. Liu, T. Wang, X. Wang, and S. Yang, "Correlation between microstructures and mechanical properties of high-speed friction stir welded aluminum hollow extrusions subjected to axial forces," *J. Mater. Sci. Technol.*, vol. 34, no. 1, pp. 102–111, 2018, doi: 10.1016/j.jmst.2017.11.015.
- [47] T. Kawasaki, T. Makino, K. Masai, H. Ohba, Y. Ina, and M. Ezumi, "Application of friction stir welding to construction of railway vehicles," *JSME Int. Journal, Ser. A Solid Mech. Mater. Eng.*, vol. 47, no. 3, pp. 502–511, 2004, doi: 10.1299/jsmea.47.502.
- [48] Y. X. Huang, L. Wan, S. X. Lv, and J. C. Feng, "Novel design of tool for joining hollow extrusion by friction stir welding," *Sci. Technol. Weld. Join.*, vol. 18, no. 3, pp. 239–246, 2013, doi: 10.1179/1362171812Y.0000000096.
- [49] S. H. y F. F. Betancourt D, "Eficiencia mecánica en la soldadura por fricción agitación de la aleación de magnesio AZ31B Mechanical efficiency in the friction stir welding of magnesium alloy AZ31B," *Redalyc*, vol. 30, no. 1, pp. 23–30, 2012.
- [50] J. D. Escobar, E. Velásquez, T. F. A. Santos, A. J. Ramirez, and D. López, "Improvement of cavitation erosion resistance of a duplex stainless steel through friction stir processing (FSP)," *Wear*, vol. 297, no. 1–2, pp. 998–1005, 2013, doi: 10.1016/j.wear.2012.10.005.
- [51] R. J. Rodríguez, C. A. Caballis, M. M. Cely B., and J. Unfried-Silgado, "A comparative study of corrosion resistance in welded joints of aluminium alloy AA1100 obtained by friction-stir and gas metal arc welding processes | Estudio comparativo de la



- resistencia a la corrosión en juntas soldadas por fricción-agitación y por el,” *Ingeniare*, vol. 26, no. 3, pp. 419–429, 2018, doi: 10.4067/S0718-33052018000300419.
- [52] D. S. Villa-salazar, D. A. Hincapié-zuluaga, M. Sc, and C. Física, “Herramientas usadas en soldadura por fricción-agitación Computer Simulation of Heat Transfer on Tools Used in Friction Stir Welding,” vol. 26, no. 2, 2015, doi: 2145 - 8456.
- [53] Hitachi, “What is Optical Emission Spectroscopy (OES)?,” *Blogs*, 2017. [https://hha.hitachi-hightech.com/en/blogs-events/blogs/2017/10/25/optical-emission-spectroscopy-\(oes\)/](https://hha.hitachi-hightech.com/en/blogs-events/blogs/2017/10/25/optical-emission-spectroscopy-(oes)/) (accessed Sep. 18, 2020).
- [54] F. Arias, “El Valle de Aburrá tiene 3,72 millones de personas,” *El Colombiano*, p. 1, Jul. 09, 2019.
- [55] The Aluminum Association Inc., “Aluminum Alloys 101,” *Industry standards*, 2019. <https://www.aluminum.org/resources/industry-standards/aluminum-alloys-101> (accessed Feb. 21, 2021).
- [56] Aalco, “6005A - T6 Extrusion,” *Literature & Datasheets*, 2019. [http://www.aalco.co.uk/datasheets/Aluminium-Alloy-6005A-T6-Extrusion\\_157.ashx](http://www.aalco.co.uk/datasheets/Aluminium-Alloy-6005A-T6-Extrusion_157.ashx).
- [57] Aalco, “6060 - T5 Extrusions,” *Literature & Datasheets*, 2019. [http://www.aalco.co.uk/datasheets/Aluminium-Alloy-6060-T5--Extrusions\\_144.ashx](http://www.aalco.co.uk/datasheets/Aluminium-Alloy-6060-T5--Extrusions_144.ashx).
- [58] Aalco, “6101 - T6 Extrusions,” *Literature & Datasheets*, 2019. [http://www.aalco.co.uk/datasheets/Aluminium-Alloy-6101-T6-Extrusions-Bar\\_356.ashx](http://www.aalco.co.uk/datasheets/Aluminium-Alloy-6101-T6-Extrusions-Bar_356.ashx).
- [59] Aalco, “6063 - ‘0’ Extrusions,” *Literature & Datasheets*, 2019. .
- [60] Aalco, “6005A - T6 Extrusion,” *Literature & Datasheets*, 2019. .
- [61] R. Goncalves, *Introducción al análisis de esfuerzos*, Tercera. Caracas: Editorial Equinoccio, 2011.
- [62] MatWeb, “AA 6063 - T6,” *6000 Series Aluminum Alloy*, 2020. <http://www.matweb.com/search/DataSheet.aspx?MatGUID=333b3a557aeb49b2b17266558e5d0dc0>.
- [63] MatWeb, “AA 7075 - T6,” *7000 Series Aluminum Alloy*, 2020. <http://www.matweb.com/search/DataSheet.aspx?MatGUID=9852e9cdc3d4466ea9f111f3f0025c7d>.
- [64] G. T. Méndez, R. Cuamatzi-meléndez, A. A. Hernández, and S. I. Capula-colindres,

- “Correlation of Stress Concentration Factors for T-Welded Connections – Finite Element Simulations and Fatigue Behavior,” vol. 22, no. 2, pp. 194–206, 2017.
- [65] A. Chattopadhyay, G. Glinka, J. Qian, and R. Formas, “STRESS ANALYSIS and FATIGUE of welded structures,” pp. 2–21, 2011.
- [66] MatWeb, “AA 6082 - T6,” *6000 Series Aluminum Alloy*, 2020. <http://www.matweb.com/search/DataSheet.aspx?MatGUID=fad29be6e64d4e95a241690f1f6e1eb7>.
- [67] E. Jaramillo, “IMPLEMENTATION ASSESSMENT OF FRICTION STIR WELDING ( FSW ) IN THE COLOMBIAN RAIL TRANSPORT SECTOR,” University EIA, 2020.
- [68] Y. Li, L. E. Murr, and J. C. McClure, “Flow visualization and residual microstructures associated with the friction-stir welding of 2024 aluminum to 6061 aluminum,” *Mater. Sci. Eng. A*, vol. 271, no. 1–2, pp. 213–223, 1999, doi: 10.1016/S0921-5093(99)00204-X.
- [69] M. Guerra, C. Schmidt, J. C. McClure, L. E. Murr, and A. C. Nunes, “Flow patterns during friction stir welding,” vol. 49, pp. 95–101, 2003, doi: 10.1016/S1044-5803(02)00362-5.
- [70] MatWeb, “Aluminum 6082-T4,” *6000 Series Aluminum Alloy*, 2020. <http://www.matweb.com/search/DataSheet.aspx?MatGUID=117e133f428e40949528be5a86250108> (accessed Feb. 21, 2021).
- [71] D. L. Porter and T. C. Totemeier, *Mechanical properties of metals and alloys*. Springer, 2003.
- [72] A. Bhaduri, *Mechanical Properties and Working of Metals and Alloys*, vol. 264. 2018.
- [73] A. da S. Scari, B. C. Pockszevnicki, J. Landre Junior, and P. A. A. Magalhaes Junior, “Stress-Strain Compression of AA6082-T6 Aluminum Alloy at Room Temperature,” *J. Struct.*, vol. 2014, pp. 1–7, 2014, doi: 10.1155/2014/387680.